

TRENDS IN AIR TEMPERATURE AND SEA ICE IN THE ATLANTIC LARGE AQUATIC BASIN AND ADJOINING AREAS

I.K. Peterson and R. Pettipas

Ocean and Ecosystem Sciences Division
Maritimes Region
Fisheries and Oceans Canada

Bedford Institute of Oceanography
P.O. Box 1006
Dartmouth, Nova Scotia
Canada B2Y 4A2

2013

**Canadian Technical Report of
Hydrography and Ocean Sciences 290**



Fisheries and Oceans
Canada

Pêches et Océans
Canada

Canada

Canadian Technical Report of Hydrography and Ocean Sciences

Technical reports contain scientific and technical information of a type that represents a contribution to existing knowledge but which is not normally found in the primary literature. The subject matter is generally related to programs and interests of the Oceans and Science sectors of Fisheries and Oceans Canada.

Technical reports may be cited as full publications. The correct citation appears above the abstract of each report. Each report is abstracted in the data base *Aquatic Sciences and Fisheries Abstracts*.

Technical reports are produced regionally but are numbered nationally. Requests for individual reports will be filled by the issuing establishment listed on the front cover and title page.

Regional and headquarters establishments of Ocean Science and Surveys ceased publication of their various report series as of December 1981. A complete listing of these publications and the last number issued under each title are published in the *Canadian Journal of Fisheries and Aquatic Sciences*, Volume 38: Index to Publications 1981. The current series began with Report Number 1 in January 1982.

Rapport technique canadien sur l'hydrographie et les sciences océaniques

Les rapports techniques contiennent des renseignements scientifiques et techniques qui constituent une contribution aux connaissances actuelles mais que l'on ne trouve pas normalement dans les revues scientifiques. Le sujet est généralement rattaché aux programmes et intérêts des secteurs des Océans et des Sciences de Pêches et Océans Canada.

Les rapports techniques peuvent être cités comme des publications à part entière. Le titre exact figure au-dessus du résumé de chaque rapport. Les rapports techniques sont résumés dans la base de données *Résumés des sciences aquatiques et halieutiques*.

Les rapports techniques sont produits à l'échelon régional, mais numérotés à l'échelon national. Les demandes de rapports seront satisfaites par l'établissement auteur dont le nom figure sur la couverture et la page de titre.

Les établissements de l'ancien secteur des Sciences et Levés océaniques dans les régions et à l'administration centrale ont cessé de publier leurs diverses séries de rapports en décembre 1981. Vous trouverez dans l'index des publications du volume 38 du *Journal canadien des sciences halieutiques et aquatiques*, la liste de ces publications ainsi que le dernier numéro paru dans chaque catégorie. La nouvelle série a commencé avec la publication du rapport numéro 1 en janvier 1982.

**Canadian Technical Report of
Hydrography and Ocean Sciences 290**

2013

**TRENDS IN AIR TEMPERATURE AND SEA ICE IN THE ATLANTIC LARGE
AQUATIC BASIN AND ADJOINING AREAS**

by

I.K. Peterson and R. Pettipas

**Ocean and Ecosystem Sciences Division
Maritimes Region
Fisheries and Oceans Canada**

**Bedford Institute of Oceanography
P.O. Box 1006
Dartmouth, Nova Scotia
Canada, B2Y 4A2**

© Her Majesty the Queen in Right of Canada, 2013.

Cat. No. Fs 97-18/290E ISSN 0711-6764

Correct citation for this publication:

Peterson, I. K., and R. Pettipas. 2013. Trends In air temperature and sea ice in the Atlantic Large Aquatic Basin and adjoining areas, Can. Tech. Rep. Hydrogr. Ocean Sci. 290: v + 59 p.

TABLE OF CONTENTS

ABSTRACT	iv
RÉSUMÉ	v
1.0 INTRODUCTION	1
2.0 AIR TEMPERATURE	3
2.1 DATASETS	3
2.2 RESULTS	3
3.0 SEA ICE AREA	8
3.1 DATASETS	8
3.2 RESULTS	10
4.0 SEA ICE CONCENTRATION.....	14
5.0 FREEZE-UP AND BREAK-UP	16
6.0 SEA ICE THICKNESS	18
7.0 ICEBERGS	19
8.0 CLIMATE INDICES	22
8.1 AIR TEMPERATURE	25
8.2. SEA ICE	27
9.0 CONCLUSIONS.....	28
10.0 ACKNOWLEDGMENTS	30
11.0 REFERENCES	30
APPENDIX 1: SEASONAL AIR TEMPERATURE TIME SERIES.....	37
APPENDIX 2: EFFECT OF ICE DATA REPLACEMENT	49
APPENDIX 3: SEASONAL SEA ICE AREA TIME SERIES	52
APPENDIX 4: CLIMATE INDICES.....	57

ABSTRACT

Peterson, I.K., and R. Pettipas. 2013. Trends In air temperature and sea ice in the Atlantic Large Aquatic Basin and adjoining areas, Can. Tech. Rep. Hydrogr. Ocean Sci. 290: v + 59 p.

Air temperature and sea ice area trends in eastern Canada (the Atlantic Basin, Baffin Bay and Hudson Bay regions) are estimated for the periods of 1980-2011, 1953-2011 and 1900-2011. In general, winter air temperature variability in Labrador, Nunavut, Greenland and eastern Hudson Bay, and sea ice variability in nearby regions are dominated by interannual and decadal variations associated with the North Atlantic Oscillation (NAO). However in summer, air temperature and sea ice area are more strongly associated with the Atlantic Multidecadal Oscillation (AMO), so that they have exhibited nearly monotonic trends in the recent period (1980-2011). Air temperature trends over the past 60 years are approximately 0.1-0.2°C/decade along the Canadian East Coast south of 50°N. These trends are similar to the global mean surface temperature trend in the scientific literature of 0.13°C/decade for the past 50 years, which is widely believed to be due primarily to anthropogenic climate change.

RÉSUMÉ

Peterson, I.K., and R. Pettipas. 2013. Trends In air temperature and sea ice in the Atlantic Large Aquatic Basin and adjoining areas, Can. Tech. Rep. Hydrogr. Ocean Sci. 290: v + 59 p.

On a dégagé les tendances relatives à la température de l'air et aux glaces de mer dans la région de l'est du Canada (régions du bassin de l'Atlantique, de la baie de Baffin et de la baie d'Hudson) pour les périodes de 1980 à 2011, de 1953 à 2011 et de 1900 à 2011. En général, la variabilité des températures hivernales de l'air au Labrador, au Nunavut, au Groenland et de l'est de la baie d'Hudson ainsi que la variabilité des glaces de mer pour les régions avoisinantes sont caractérisées de variations interannuelles et décennales influencées par l'oscillation nord-atlantique. Toutefois, durant l'été, les températures de l'air et les glaces sont plus fortement influencées par l'oscillation multidéennale de l'Atlantique, à tel point qu'elles ont affiché des tendances presque monotones au cours de la période récente (1980-2011). Les tendances des températures de l'air au cours des 60 dernières années se situent à environ 0,1 à 0,2 °C par décennie le long de la côte est du Canada, au sud du 50° degré de latitude nord. Ces tendances sont semblables à la tendance de la température moyenne à la surface du globe de 0,13 °C par décennie pour les 50 dernières années qui est documentée dans divers ouvrages scientifiques et qui, de l'avis de beaucoup, serait principalement attribuable aux changements climatiques anthropiques.

1.0 INTRODUCTION

Over the last century, global surface temperature has increased by about 0.74°C, and it is believed that most of the increase in temperature since the mid-twentieth century is very likely due to the increase in anthropogenic greenhouse gas concentrations (IPCC, 2007). Decreases in snow and ice extent are consistent with warming, with a trend of -2.7% per decade in annual average Arctic sea ice extent since 1978 (IPCC, 2007). Considerable regional differences in warming trends (Fig. 1) are observed on all time scales and likely result from changes in atmospheric circulation (Solomon et al., 2007).

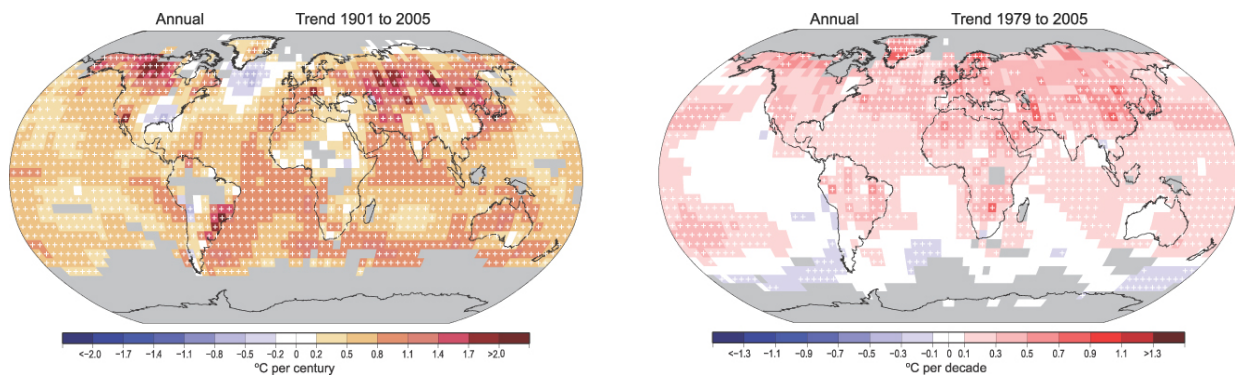


Fig. 1. Global surface temperature trends in 1901-2005 and 1979-2005 (Fig. 3-9 in Solomon et al., 2007).

This report is mainly concerned with trends of sea ice in the Atlantic Large Aquatic Basin (LAB), which is under consideration in the Aquatic Climate Change Adaptation Services Program (ACCASP) of Fisheries and Oceans Canada. However, the adjoining regions of Baffin Bay and Hudson Bay in the Arctic LAB are also included. Air temperature is also considered in the report because of its strong relationship with sea ice (Walsh and Johnson, 1979), and because relatively long accurate time series are available. Trends in iceberg numbers are included because of the high correlation with both air temperature and sea ice (Prinsenberg et al., 1997), and the potential impact of icebergs on marine operations. In this report, trends are considered for three periods: (a) since 1900, (b) since the 1950s and (c) since 1980. The map in Figure 2 shows the 17 stations used for air temperature and the 9 regions used for ice area in this report.

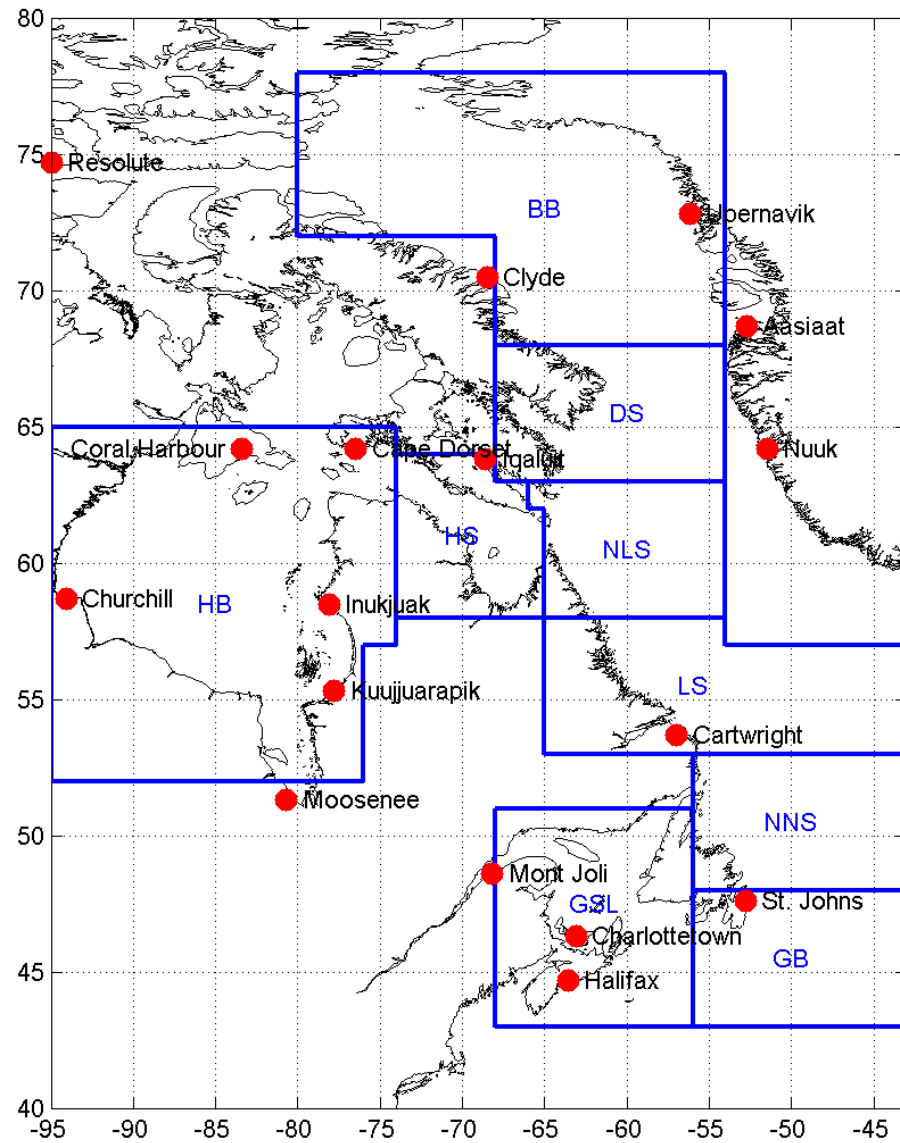


Fig. 2. Map showing locations of air temperature stations and sea ice areas.

2.0 AIR TEMPERATURE

2.1 DATASETS

Adjusted and homogenized surface air temperature records (Vincent et al., 2009, 2012) for 14 stations in eastern Canada (Fig. 2) were downloaded from <http://www.ec.gc.ca/dccha-ahccd/default.asp?lang=en&n=70E82601-1>. Monthly, seasonal and annual mean temperatures were provided until 2012, with some records extending back before 1900. Temperature records from 3 stations in Greenland from DFO's AZMP database of Climate Indices were also used in this study, but have not been adjusted and homogenized.

2.2 RESULTS

The trends for annual mean air temperature are shown for the periods 1900-2012, 1953-2012, and 1980-2012 in Figure 3, and the trends for seasonal mean air temperature in Appendix 1. The time series of annual mean air temperature are plotted in Fig. 4, and seasonal mean air temperature are plotted in Appendix 1. The p-values listed to the right of the time series plots give an indication of the statistical significance; they have not been adjusted for autocorrelation. In the absence of autocorrelation, if the p-value is less than 0.05, the null hypothesis that the trend is equal to zero can be rejected at the 5% significance level, and if the p-value is less than 0.20, the null hypothesis can be rejected at the 20% significance level. In the presence of autocorrelation due to low-frequency variability, the p-value will reflect an overestimation of the degrees of freedom, and therefore will underestimate the significance level.

For annual air temperatures, trends for the period 1900-2012 are generally consistent with Solomon et al. (2007, Fig. 3-9) (Fig. 1), with a low value of 0.03 °C/decade in southern Greenland (Nuuk). At the 4 stations in eastern Canada south of 50°N, values are 0.05-0.16 °C/decade compared to a global mean of 0.074 °C/decade for the period 1906-2005 (Solomon et al., 2007).

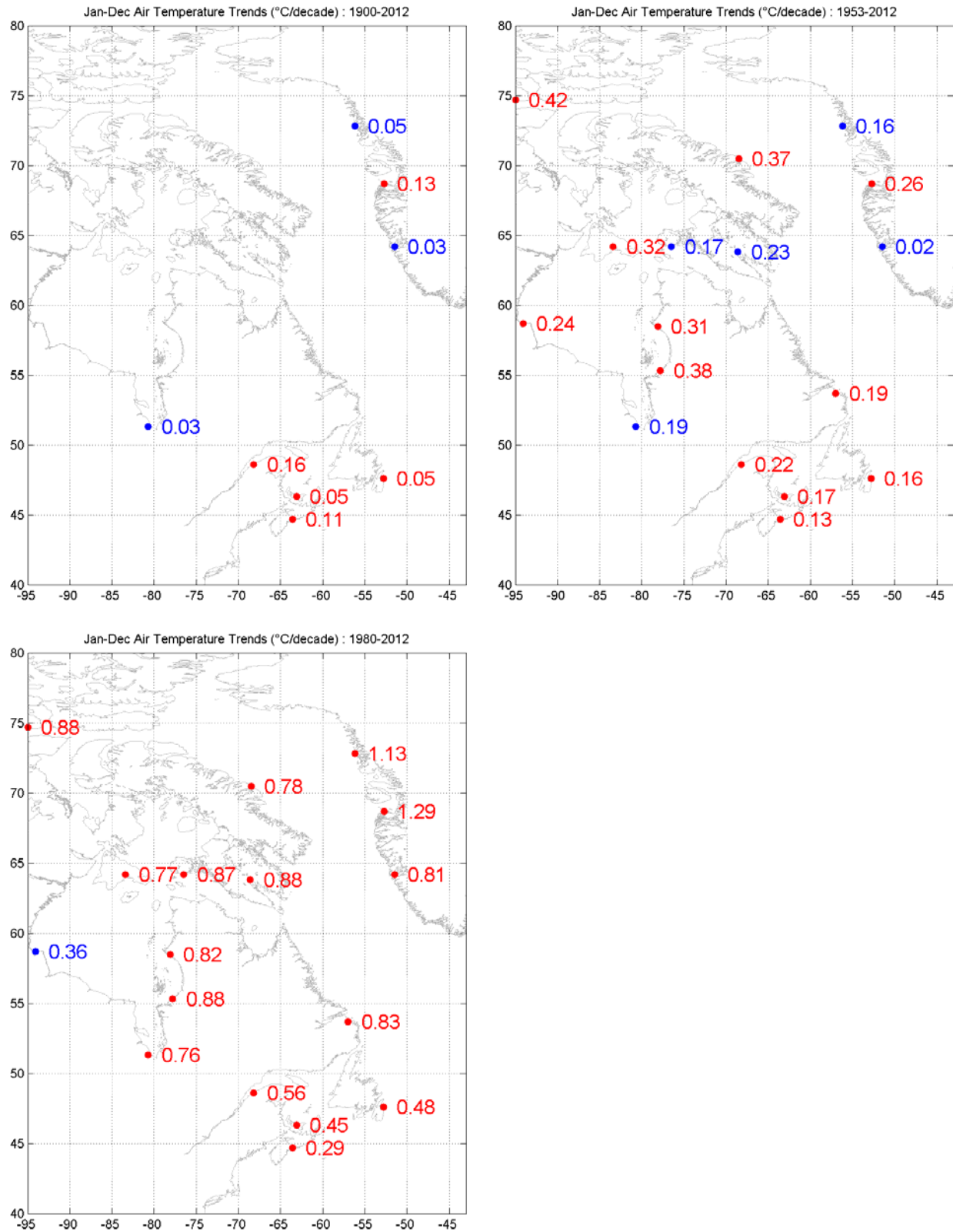


Fig. 3. Air temperature trends: red indicates trend is significant at 5% level ($p < 0.05$).

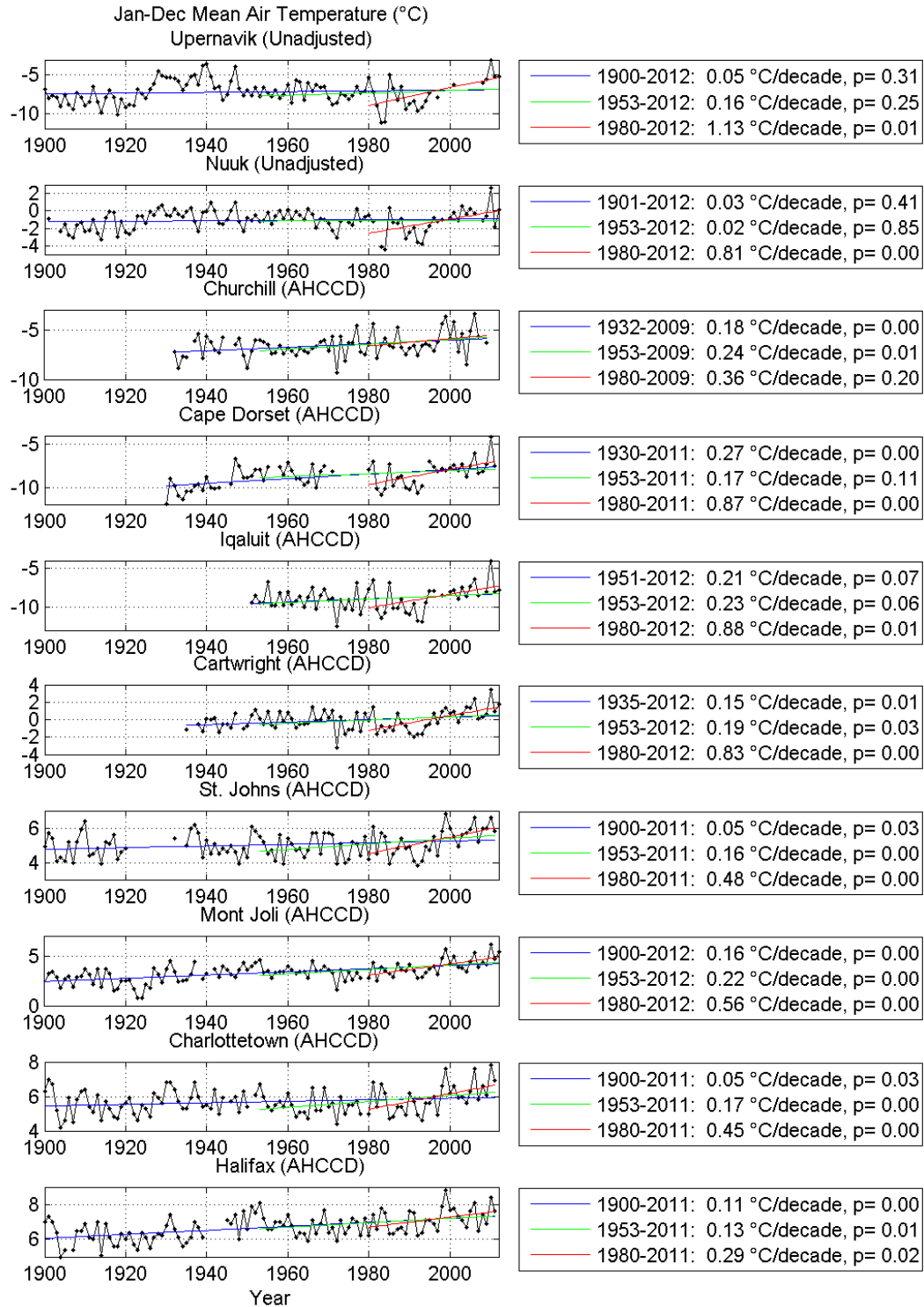


Fig. 4. Annual mean air temperatures.

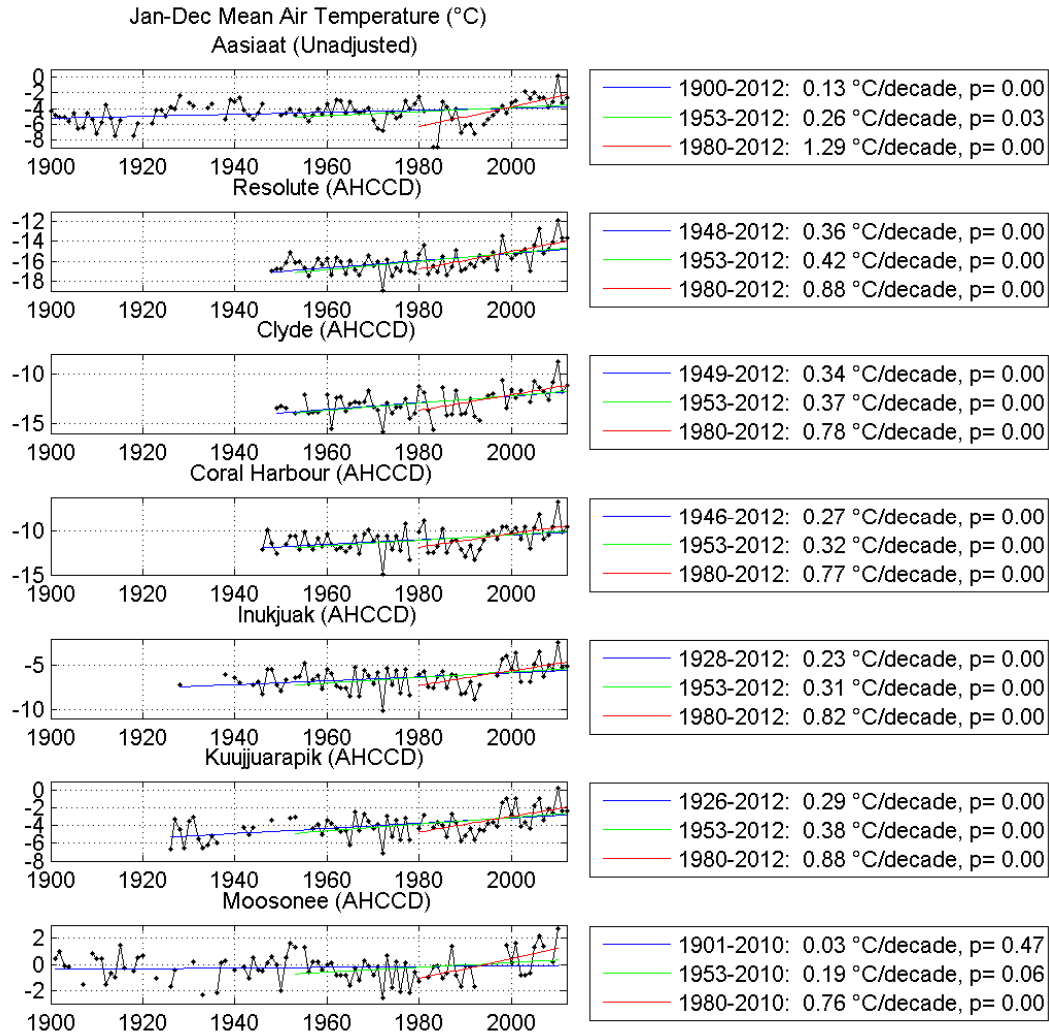


Fig. 4 (cont.)

Air temperature trends in Greenland are generally less than for the Canadian East Coast during the 1900-2012 period (Fig. 3), in agreement with the global surface temperature trend pattern for 1901-2005 (Fig. 1). Figure 1 also shows a region with negative surface temperature trends to the south of Greenland. This is also a dominant feature in the spatial pattern for the first EOF of global SST (Wang et al., 2008), and in a regression of mean surface air temperature on the global mean temperature (Drijfhout et al., 2012). It has been suggested that this “warming hole” is associated with a decline in the Atlantic

Meridional Circulation (AMOC), since climate model simulations showed a similar pattern that was more closely associated with the AMOC than with radiative forcing (Drijfhout et al., 2012). Anthropogenic forcing is projected to weaken the AMOC (Meehl et al., 2007), resulting in reduced warming, increased atmospheric stability, and decreased occurrence of polar low cyclones in the subpolar North Atlantic (Woollings et al., 2012a and b).

Trends for the period 1953-2012 (Fig. 3) are generally higher than for 1900-2012, with values of 0.13-0.22 °C/decade in eastern Canada south of 50°N, compared to a global mean of 0.13°C/decade for the period 1956-2005 (Solomon et al., 2007). The trends at Resolute and Clyde are about 0.4 °C/decade ($p < 0.05$), and trends in western Greenland and southern Baffin Island are not significant ($p > 0.05$).

In a study by Serreze and Barry (2011), the global surface air temperature trend pattern for the period 1960-2009 showed evidence of Arctic amplification, with trends of 0.4-0.8°C/decade in the western CAA, 0.2-0.4°C/decade in northern Baffin Bay, Hudson Bay, and in the Labrador/Newfoundland Slope region, and 0.1-0.2°C/decade in southeastern Canada and southern Greenland. In Figure 3, trends for the 1953-2012 period are similar.

Trends for the period 1980-2012 are generally higher than for 1953-2012 (Fig. 3) and higher than the global mean of 0.18°C/decade for the period 1981-2005 (Solomon et al., 2007), with values of 0.81 °C/decade at Nuuk, 0.88 °C/decade at Iqaluit, 0.83 °C/decade at Cartwright, 0.48 °C/decade at St. John's, and 0.29 °C/decade at Halifax. This north-to-south gradient in the trend is consistent with Fig 3-9 in Solomon et al. (2007) (Fig. 1).

For the 1900-2012 period, the seasonal trends are generally higher in the winter than in other months, and more of the trends are significant in the winter (Fig. A1-1), because of particularly low winter temperatures in 1900-1920. For Nuuk, Greenland, the trends are highest in the winter and lowest in the spring and summer, in agreement with trends for the 1901-2000 period reported by Box (2002). Trends are significant at Mont Joli for all seasons and at St. John's for summer only.

For the 1953-2012 period, most of the trends are significant in summer and autumn and few are significant in winter and spring (Fig. A1-2), because of more interannual and decadal variability in the winter and spring (Fig. A1-4, A1-5). Zhang et al. (2011) and Thistle and Caissie (2013) also found that more trends are statistically significant in summer than in other months in southeastern Canada over the last 60 years. For the 1980-2012 period, most of the seasonal trends are significant except in the spring (Fig. A1-3) when there is high interannual variability (Fig. A1-5), in agreement with Thistle and Caissie (2013).

3.0 SEA ICE AREA

3.1 DATASETS

Sea ice concentration trends are considered for the domain 40-80°N, 95-43°W and the period 1900-2011 using the HadISST1 dataset (available at <http://www.metoffice.gov.uk/hadobs/hadisst/>), which consists of mid-month sea ice concentrations on a 1° latitude by 1° longitude grid for the period 1870 to the present (Rayner et al., 2003).

For the period 1901-1978, the HadISST1 dataset is based mainly on the Walsh dataset (Walsh, 1978), consisting of end-of-month ice concentrations on a 1 degree cylindrical projection grid, derived from ice charts. For the period since 1978, passive microwave data are used; the monthly gridded data consist of the median of daily area-averaged values over the month. The passive microwave data is from the NASA Goddard Space Flight Center for the period 1978-1996, and from the NCEP operational sea ice dataset since 1997. Before 1953, much of the Walsh dataset consists of climatology (missing values replaced with a long-term mean value), with increasing amounts of observed data throughout the period. Because of these discontinuities, the HadISST dataset should be used with caution for studies of climatic trends or variability. However some corrections

are done in the HadISST dataset to increase the homogeneity of the pre- and post-1978 data (Rayner et al., 2003).

Sea ice concentration data are also available from the Canadian Ice Service Digital Archive (CISDA) at <http://www.ec.gc.ca/glaces-ice/>, in the form of digital ice charts in Arc/Info GIS E00 format (Tivy et al., 2011a). In the regional data set (CISDA-R), data are available for the Eastern Arctic, Hudson Bay and Approaches, and Canadian East Coast (south of about 55°N) regions since 1968, 1971 and 1968 respectively. For the first two regions, the dataset contains weekly data from about June to October-December, and monthly data for the rest of the year since 1980. For the third region, it contains weekly data for the entire ice season. The historical data set (CISDA-H) produced recently contains weekly data for the period 1959-1969, however many of the data are missing for the winter and spring months north of 55°N. Ice concentrations were extracted from the digital ice charts on a 10 km grid, and the concentrations were spatially averaged in 1-degree squares. Daily values were then interpolated, and monthly means calculated.

In the HadSST1 dataset, for the period when passive microwave data are used, spurious sea ice can appear around the coasts due to land contamination resulting from the relatively large footprint of the instrument (of order 50 km) (Rayner et al., 2003). This is particularly problematic during the melt season when much of the sea ice is within a grid point (1 degree) of the coast. This results in a suspect positive trend in April sea ice in southern areas for 1980-2011 (Appendix 2, Fig. A2-1), while trends in winter air temperature are also positive over the same period (Fig. A1-4). Therefore the HadISST1 data for later years were replaced with data from Canadian Ice Service (CIS) ice charts, depending on when charts are available. For the Canadian East Coast region south of 53°N, data were replaced after 1960. For Eastern Arctic and Hudson Bay and Approaches, data were replaced for July-September after 1968, and for October-June after 1980. As a result, the trend in April sea ice for 1980-2011 is now negative, as expected (Appendix 2, Fig. A2-2).

3.2 RESULTS

Time series and trends of annual mean sea-ice area for the areas indicated in Fig. 2 are shown in Fig. 5, and plots for seasonal mean ice-area are shown in Appendix 3. Constant values for sea ice area prior to 1953 are often found because of replacement of missing data with a long-term mean value in the Walsh dataset. Therefore, there is high uncertainty associated with the data prior to 1953.

The annual and seasonal trends for the 1953-2011 and 1980-2011 periods are listed in Table 1. For annual mean ice areas (Fig. 5), the trends over the 1953-2011 period are generally small (-3 to -1% per decade) and not significant at the 5% level. For the 1980-2011 period, the trends range from -4% per decade in the north in Baffin Bay and Hudson Bay, to -16% per decade in the Gulf of St. Lawrence, and -20% per decade on the Northeast Newfoundland Shelf, and are all significant ($p < 0.05$). The time series plots for Davis Strait and the northern Labrador Sea show peaks at about 1972, 1983-84, and 1990-93, and 2008-09. Farther south on the NE Newfoundland Shelf, the peaks are at 1972-74, 1984-85, 1991-1994, and 2008-09, consistent with Deser et al. (2002).

Corresponding troughs can be seen in the winter air temperature records for Iqaluit and Cartwright in these years (Fig. A1-4). In the Gulf of St. Lawrence, the 1980s and 1990s ice area peaks are blended into a single peak, as are the winter air temperature troughs at St. John's and Charlottetown. In 2003, there is also an ice area peak in the Gulf of St. Lawrence, and winter air temperature troughs at St. John's and Charlottetown (Fig. A1-4).

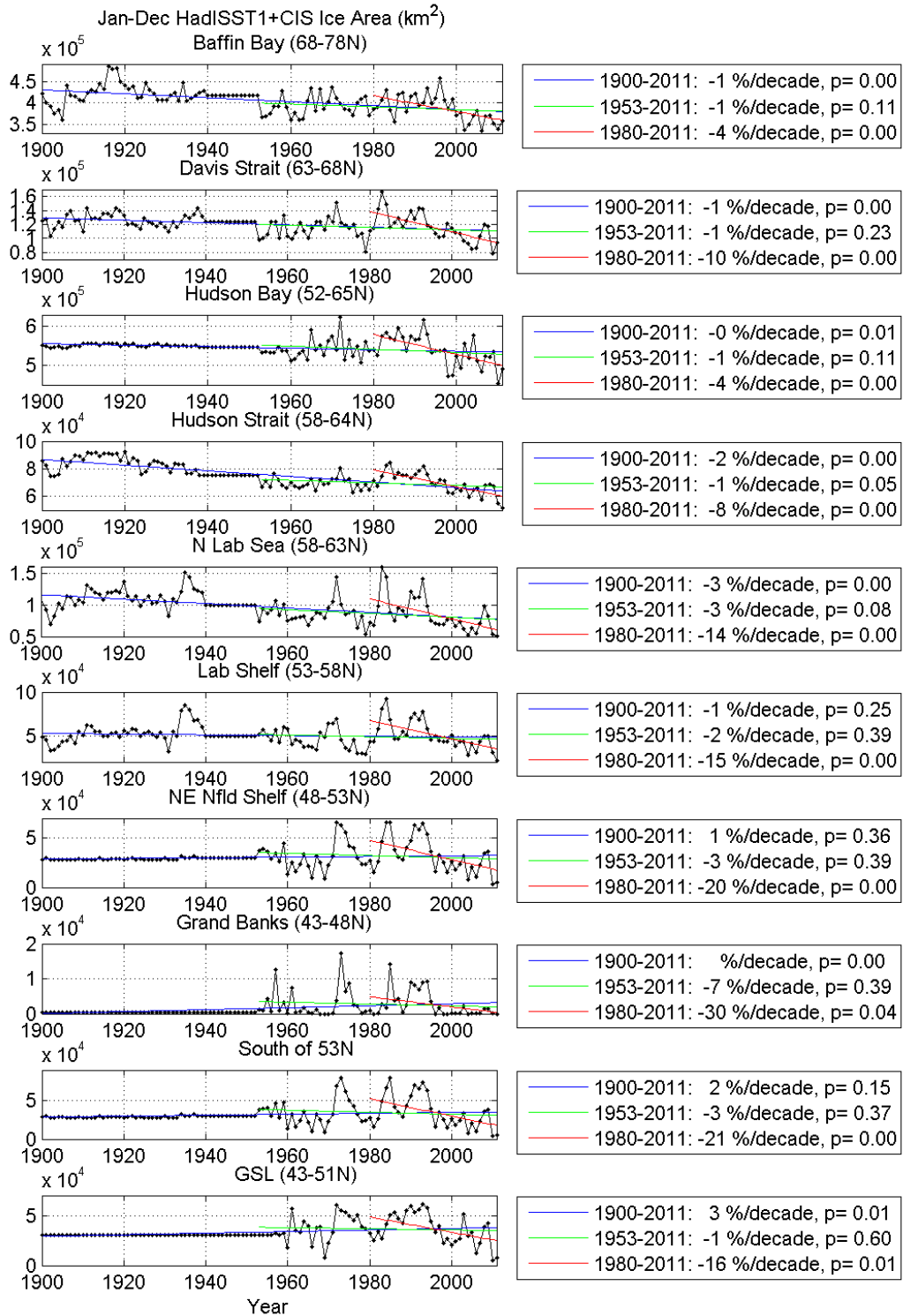


Fig. 5. Annual mean ice area.

Table 1. Ice area trends for 1953-2011 and 1980-2011 (annual, winter, spring and summer means) for Baffin Bay (BB), Davis Strait (DS), Hudson Bay (HB), Hudson Strait (HS), Northern Labrador Sea (NLS), Labrador Shelf (LS), Northeast Newfoundland Shelf (NENS), Grand Banks (GB), South of 53°N (S53), and Gulf of St. Lawrence (GSL). An asterisk indicates the trend is significant at the 5% level.

	1953-2011					1980-2011				
	Ann	Wi	Sp	Su	Au	Ann	Wi	Sp	Su	Au
BB	-1	-0*	-0	-7*	0	-4*	-1*	-3*	-17*	-6*
DS	-1	1	-1	-10*	-1	-10*	-7*	-7*	-24*	-17*
HB	-1	-0	-1*	-5	-0	-4*	-0	-3*	-19*	-13*
HS	-1 *	1*	-2*	-10*	-3	-8*	-1	-6*	-31*	-19*
NLS	-3	-1	-4*	-29*	-5	-14*	-10*	-14*	-29*	-26*
LS	-2	0	-4	-18*	12	-15*	-12*	-17*	-31	-29*
NENS	-3	-1	-7	-14	1	-20*	-20*	-20*	-33	-35*
GB	-7	-7	-10	n/a	-5	-30*	-31*	-16	n/a	n/a
S53	-3	-2	-7	-33	1	-21*	-21*	-20*	-33	-35*
GSL	-1	-1	-5	-29	-8	-16*	-15*	-17	-29	-32*

For the 1953-2011 period, the temporal patterns for the winter months (Fig. A3-1) are similar to those for the annual mean, and most trends are not significant at the 5% level. This is also true for the spring and autumn months (Fig. A3-2, A3-4), except in Hudson Bay, Hudson Strait and the northern Labrador Sea in the spring, where decreases in ice area are small but significant ($p < 0.05$); however this may be due to higher uncertainty in the spring data north of 55°N prior to the 1980s. In the summer (Fig. A3-3), decreases in ice area are generally significant ($p < 0.05$) in all areas where ice was present. The trends decrease from -7% per decade in Baffin Bay, to -10% per decade in Davis Strait, and -14% per decade in the northern Labrador Sea. For the 1980-2011 period, most trends are significant in all seasons, for all areas where ice was present, and are lower (more negative) than for 1953-2011. The summer trends are -17, -24 and -29% per decade for Baffin Bay, Davis Strait and the northern Labrador Sea respectively.

Trends of summer sea ice area in various regions of the Arctic and Hudson Bay and Approaches domains were reported by Tivy et al. (2011a, 2011b) for the period 1968-

2008, based on digital ice charts produced by the Canadian Ice Service. The trends were recently updated for the period 1968-2010 (Henry, 2011), and were -10 % per decade for the Baffin Bay region (25 June -15 October), and -11, -16, -14 and -17 % per decade for the Hudson Bay, Hudson Strait, Davis Strait and Northern Labrador Sea regions respectively (18 June -19 November). All the trends were statistically significant at the 5% level or below.

Figure 6 shows the updated time series for the Baffin Bay, Davis Strait and the Northern Labrador Sea regions (1968-2012), as well as 3 sub-regions in the Canadian East Coast region (Southern Labrador Sea/East Newfoundland Waters, Gulf of St. Lawrence and the Scotian Shelf). The ice areas for the first 3 sub-regions were obtained from the IceGraph Tool on the CIS website, extended back to 1968 from 1971 using the CIS historical charts. The values are slightly lower than those shown in Henry (2011), possibly because ice in “Open Water” and “Bergy Water” areas is not included in the IceGraph dataset. Therefore the trends are somewhat higher for the total period (-12, -16 and -20% per decade; 1968-2012) compared to -10, -14 and -17% per decade; 1968-2010 from Henry (2011)). The ice area trends for the 4 northern sub-regions for the period 1968-2012 are all significant ($p < 0.05$), while the trends for the Gulf of St. Lawrence and Scotian Shelf are not significant for the 1963-2012 period ($p > 0.05$). The trends for all sub-regions are significant for the 1983-2012 period ($p < 0.05$).

Trends of annual-mean and seasonal-mean sea ice extent and area in various regions of the northern hemisphere were reported by Cavalieri and Parkinson (2012) for the period 1979-2010, based on passive microwave data. The trends were -6, -9, and -10% per decade for Hudson Bay, Baffin Bay/Labrador Sea and the Gulf of St. Lawrence for annual-mean sea ice extent, which was calculated using a concentration threshold of 15%. The trends were statistically significant at the 1% level for the first two regions, and at the 5% level for the Gulf of St. Lawrence. This is in general agreement with annual trends in ice area for the 1980-2011 period shown in Figure 5.

Extremely low values of sea ice extent were also reported off Newfoundland and Labrador for recent years (Colbourne et al., 2011), and sea-ice volume was at a record-low in 2010 in the Gulf of St. Lawrence (Galbraith et al., 2011) and at a second-lowest value on the Scotian Shelf (Hebert et al., 2011).

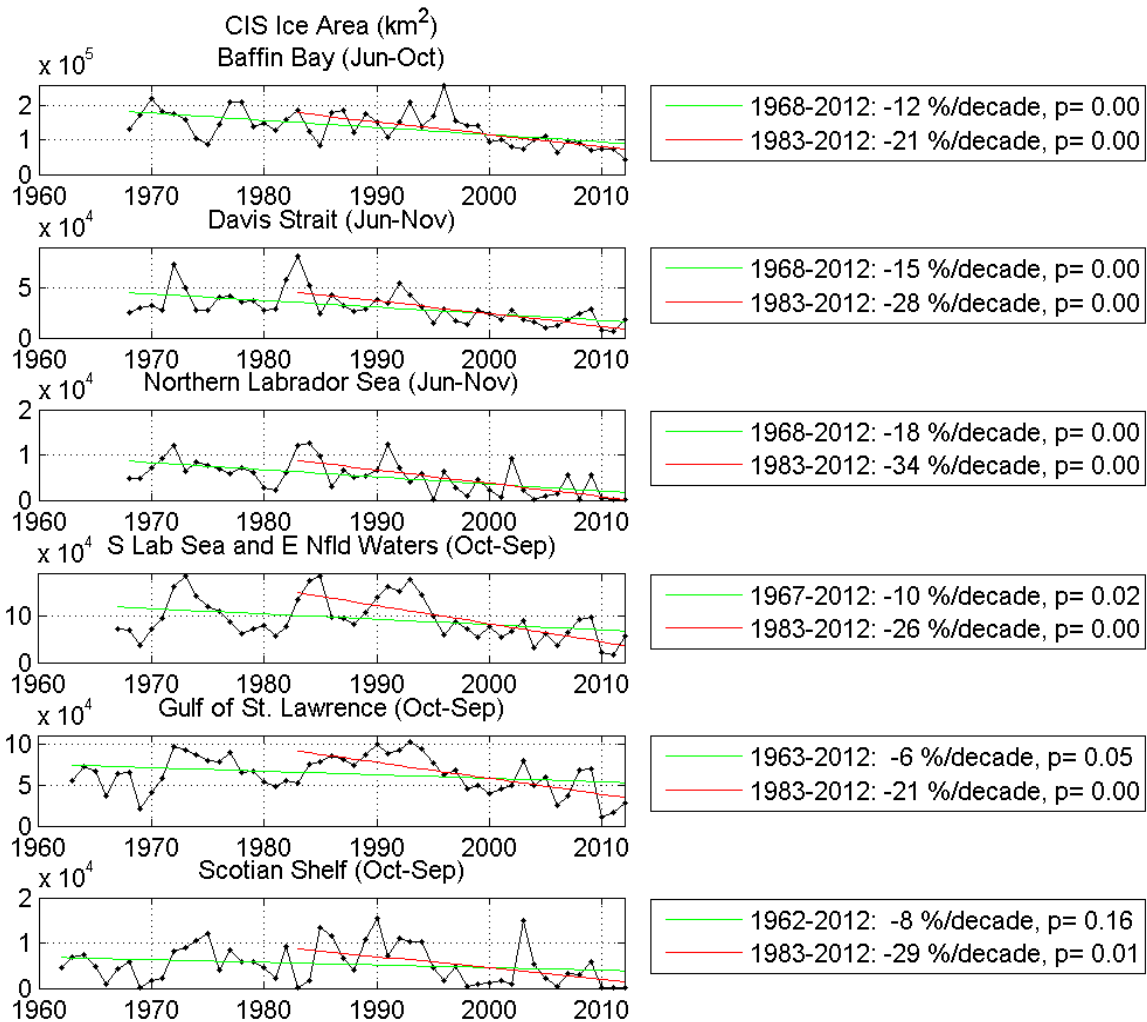


Fig. 6. Sea ice area and trends derived from the CIS dataset.

4.0 SEA ICE CONCENTRATION

The difference in sea ice concentration (SIC) trends between seasons can also be seen in 25-year averaged SIC in March and July for 1961-1985 and 1986-2010 (Fig. 7). There

is little apparent difference in ice coverage between the 2 periods for March. For July, a decreasing trend is more apparent, particularly in Baffin Bay.

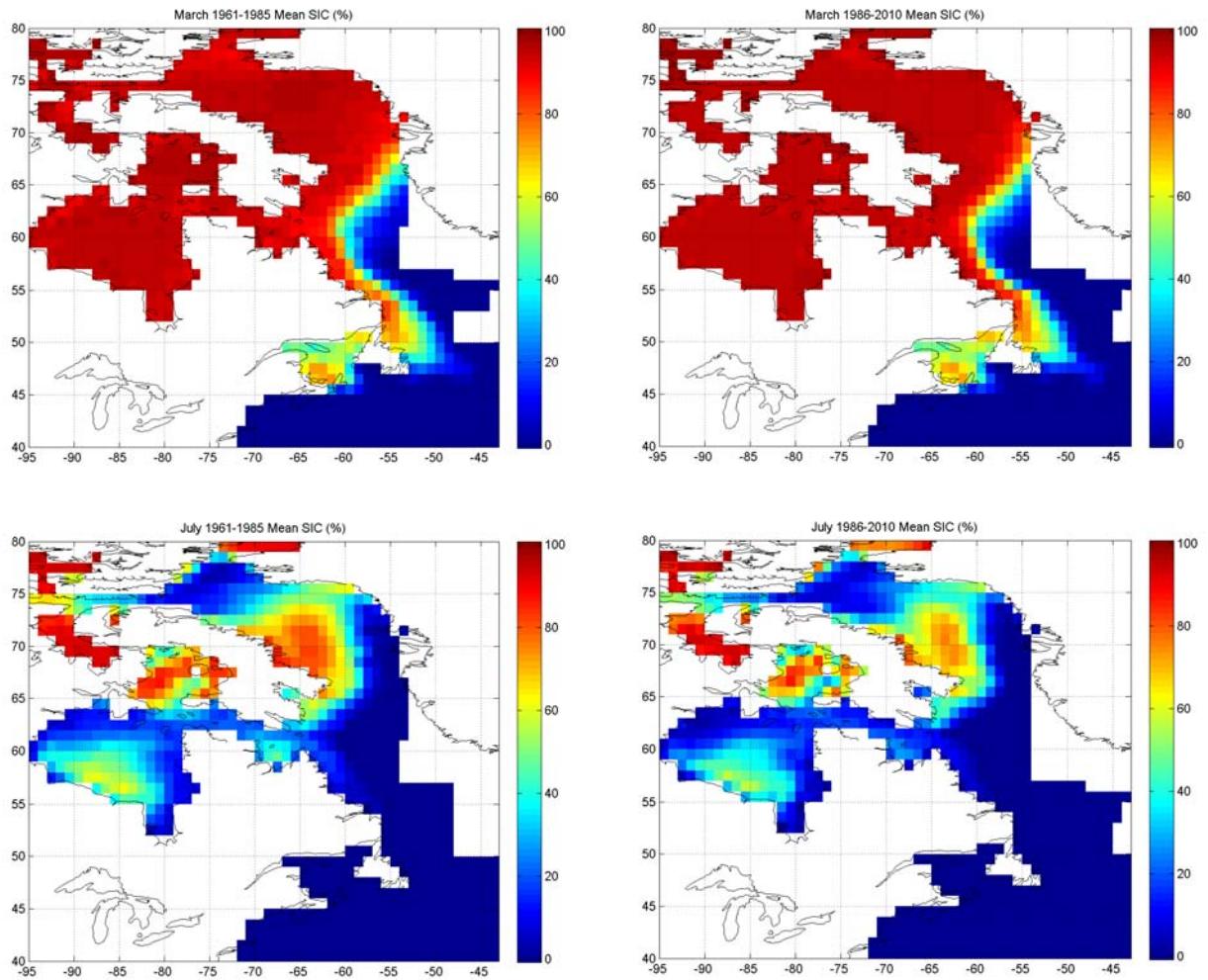


Fig. 7. 25-year mean sea ice concentration (SIC) for March (top row) and July (bottom row) for 1961-1985 (left) and 1986-2010 (right).

The mean and trend of annual mean sea ice concentration (SIC) are shown for the period 1980-2011 (Fig. 8). Generally trends are highest in areas of strong SIC gradients where a general retreat of the ice edge would have the largest impact.

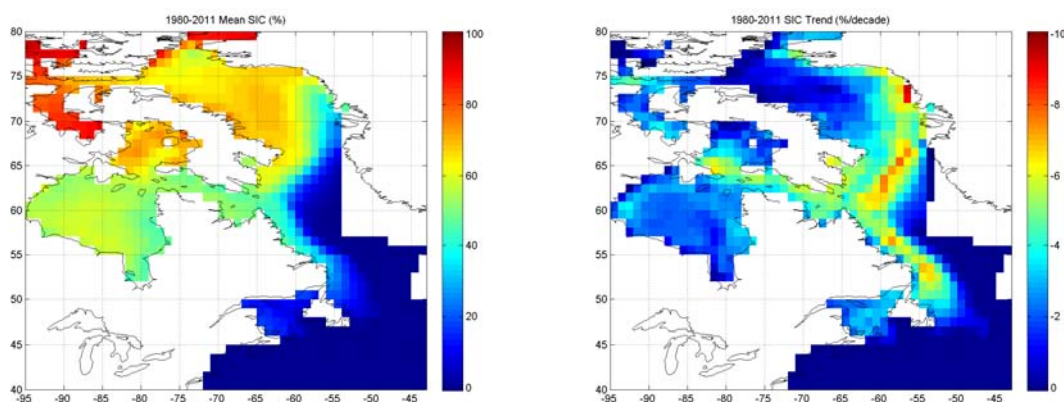


Fig. 8. Mean and trend of annual mean sea ice concentration (SIC), 1980-2011 from CIS data.

5.0 FREEZE-UP AND BREAKUP

Crane (1978) examined sea ice retreat and advance in the Davis Strait-Labrador Sea area for the years 1964-1974, and concluded that early retreat is associated with an increased frequency of southerly airflow, and early advance is associated with an increased frequency of northerly and westerly flow. However years of early ice advance corresponded to years of late retreat in 3 out of the 5 heaviest ice years, and years of late ice advance corresponded to years of early retreat in 4 out of the 6 lightest ice years. With an early ice retreat, the ocean would warm for a longer period, resulting in high ocean heat content and late ice advance (or freeze-up) in the autumn.

Markus et al. (2009) reported trends in melt and freeze onset days and melt season length for the northern hemisphere for the period 1979-2006 from passive microwave data. For the Hudson Bay and Baffin Bay/ Labrador Sea regions, the trends were -5 and -3 days/decade respectively for the first day of continuous melt (i.e. earlier), 5 and 3 days/decade for the first day of continuous freeze (i.e. later), and 10 and 6 days/decade for the melt season length (i.e. longer). These trends were all significant at the 5% level or less. Similarly, trends in ice break-up dates from CIS ice chart data were -5, -6 and -3

days per decade for Foxe Basin, Hudson Strait and Hudson Bay for the period 1971-2009 (Galbraith and Larouche, 2011).

Trends in the days of first and last ice appearance from CIS data in the Canadian East Coast region for the periods of 1963-2011 and 1980-2011 are shown in Fig. 9. Trends are highest for the latter period, in agreement with sea ice and air temperature trends. For 1980-2011, trends in the day of last appearance are stronger east of Labrador than to the south in the Gulf of St. Lawrence and east of Newfoundland, in agreement with stronger air temperature and sea ice trends in the summer than in the spring.

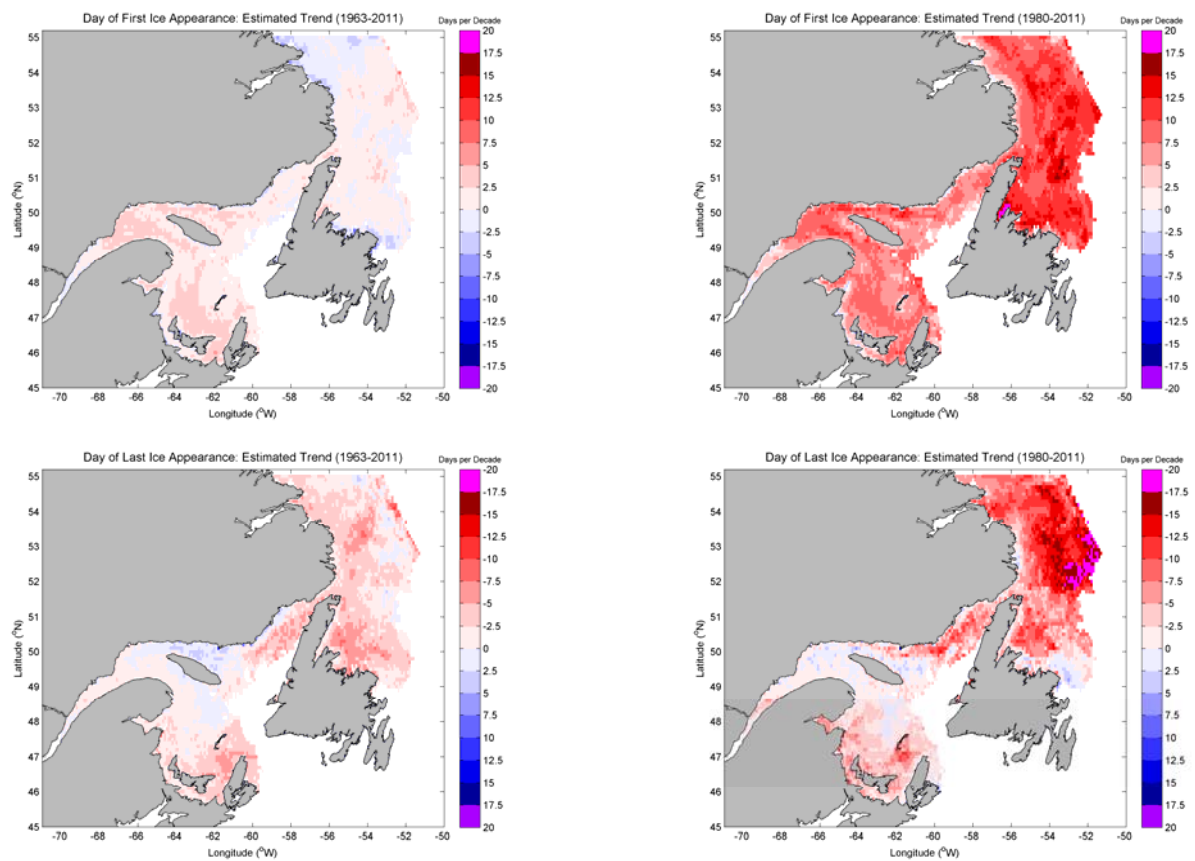


Fig.9. Trends in first appearance (top row) and last appearance (bottom row) for 1963-2011 (left) and 1980-2011 (right).

6.0 SEA ICE THICKNESS

Sea ice thickness data in the Baffin Bay/Atlantic Basin area are relatively sparse, or extend over a period too short to infer meaningful trends. Sea ice draft was measured with a moored upward-looking sonar on the Labrador shelf (Makkovik Bank) every second year between 2003 and 2011 (Peterson et al., 2013). The two years with relatively low mean ice draft (2005 and 2011), also had low ice duration periods, and high air temperatures when ice was not present. Sea ice thickness has also been measured using a helicopter-borne EM system in most years in the southern Gulf of St. Lawrence since 1996, and off Labrador in several years since the early 1990s (Peterson et al., 2003; Prinsenberg et al., 2012).

Wadhams et al. (1985) measured a mean ice draft of 1.05 m in central Davis Strait from submarine sonar profiles in February 1967. In comparison, Wu et al. (2013) give mean values of 1.0m and 2.1m in January-March 2007 and 2008 from moored upward-looking sonar measurements at C2, also in central Davis Strait. Air temperatures in the winter of 2007-2008 are unusually low, and lower than in the winter of 2006-2007 (Vage et al., 2009). Ice thickness is about 13% higher than ice draft, for a salinity of 33 psu, a temperature of -1.8°C , and an ice density of 0.91 Mg m^{-3} .

Landfast ice thickness and duration are simulated for the years 1969-1979 using a one-dimensional model at ten northern Canadian stations including Clyde, Resolute, Coral Harbour, Iqaluit and Cartwright (Dumas et al., 2006). The correlations with observed values are significant in most cases ($p < 0.05$). Projections of ice thickness and duration for 2041-60 and 2081-2100 using the Canadian Centre for Climate Modelling and Analysis global climate model (CGCM2) indicate decreases at all stations except Cartwright. Increases are projected at Cartwright due to increased ice-snow formation associated with increased snowfall, and to slight cooling along the Labrador coast associated with reduced deep ocean convection (Dumas et al., 2006). However, more

recent models are not thought to show cooling along the Labrador coast, so there is high uncertainty associated with the Cartwright projection.

Thus there is evidence that low ice thickness or draft is associated with high air temperature for pack ice in Baffin Bay and on the Labrador Shelf, and for landfast ice in many northern locations. Snow thickness also has a major effect of landfast ice thickness.

7.0 ICEBERGS

A dataset of the monthly number of icebergs drifting south of 48°N since 1900 has been produced by the International Ice Patrol (IIP) (Anderson, 1993). It is well known that iceberg numbers are highly correlated with sea ice extent off Newfoundland (Smith, 1931; Prinsenberget al., 1997). With respect to atmospheric SLP gradients, icebergs are most highly correlated with the winter SLP gradient across the Labrador Sea (Smith, 1931), in agreement with a more recent study showing that with respect to surface winds, icebergs are most highly correlated with northwesterly winds in the central Labrador Sea (Peterson et al., 2000).

The annual iceberg flux, i.e. the number of icebergs drifting south of 48°N (Fig. 10), and air temperature at St. John's (Fig. 4) show similar fluctuations since 1900. Although the iceberg flux in the last 20-30 years has generally been high, this is probably due to changes over time in methods of data collection and in the information provided in the database (Peterson, 2004). Thus the decreasing trend of -6/decade in the square root of the annual iceberg flux over the last 30 years (Fig. 10) probably represents an underestimate. The trend for the 1900-2011 period is not significant at the 5% level ($p=0.32$).

The iceberg season length (Fig. 10) was calculated as the total number of months with an iceberg flux greater than zero. The iceberg season length appears to have a decreasing trend since 1900, consistent with an increasing air temperature trend. The iceberg

season length appears to be particularly high between 1900 and the mid-1920s, in agreement with ice extent off Newfoundland from Hill (1999) (Fig. 11). However it is possible that for both time series, the trend is due in part to changes in observational technology over time. For the period since the late 1950s, ice extent from Hill (1999) (Fig. 11) shows similar fluctuations to those for ice area south of 53°N for winter and spring (Fig A3-1, A3-2), as both datasets are based on CIS ice charts during this period.

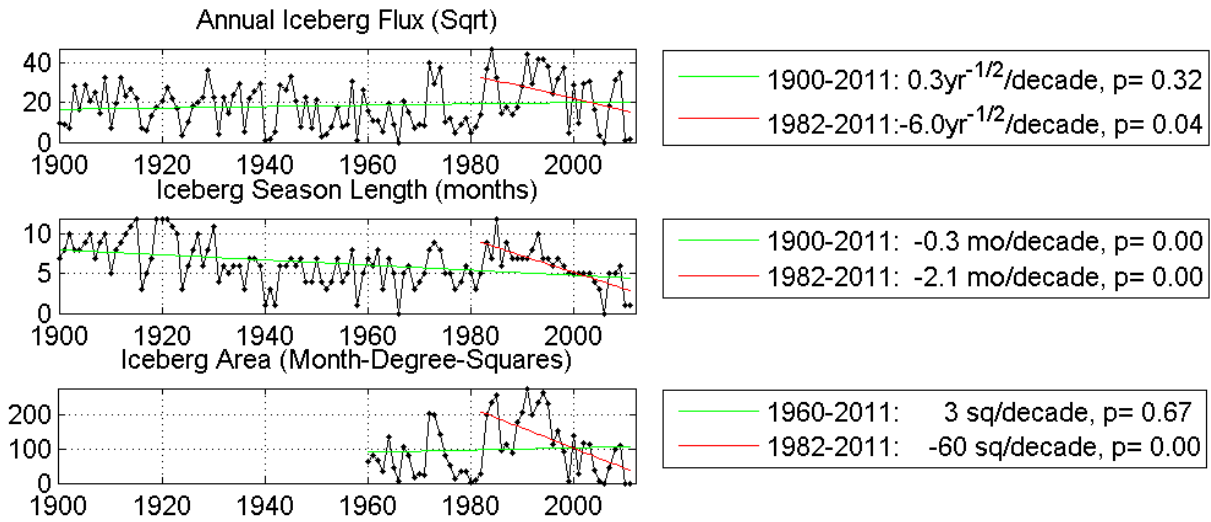


Fig. 10. The annual number of icebergs drifting south of 48°N (top panel), iceberg season length (middle panel), and the iceberg area, represented by the total number of latitude-longitude degree squares south of 48°N where icebergs have been sighted in each month, integrated over all months of the year (bottom panel).

The IIP iceberg sighting database contains the locations of sightings of individual icebergs since 1960 (Anderson, 1993). Iceberg area was calculated as the total number of latitude-longitude degree squares south of 48°N where icebergs have been sighted in each month, integrated over all months of the year (Fig. 10). The iceberg area shows similar fluctuations to the iceberg flux, however there is a clearer decrease in iceberg area than iceberg flux since the mid-1990s.

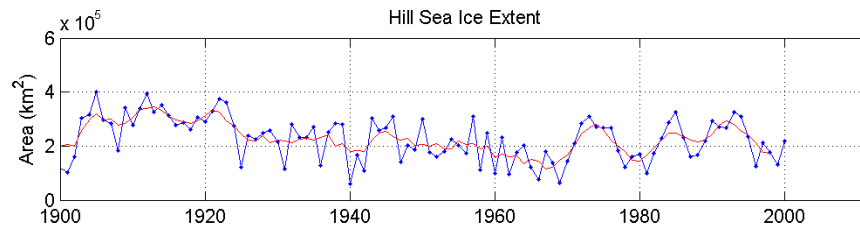


Fig. 11. The ice extent off Newfoundland from Hill (1999), available at <http://researchers.imd.nrc.ca/~hillb/index.html>).

The occurrence of icebergs from Baffin Bay to the Grand Banks may also be affected by ice discharge from Greenland glaciers (i.e. dynamic ice loss). This would be expected to increase with air temperature, while iceberg deterioration would also increase with air temperature. For the 18 year period 1992-2009, ice discharge increased by 9.0 Gt/yr^2 (Rignot et al., 2011), which represents about 18% per decade. Glacier acceleration occurred south of 66°N between 1996 and 2000, and expanded to 70°N in 2005 (Rignot and Kanagaratnam, 2006). It has been suggested that the acceleration is due to increased lubrication of the ice-bedrock interface, weakening of the floating ice tongue buttressing the glacier, and more recently, a sudden increase in subsurface ocean temperature (Holland et al., 2008). Digital elevation models for northwestern Greenland derived from aerial photographs dating back to the mid 1980s suggest that there have been two independent dynamic ice loss events: in 1985-1993 and 2005-2010 (Kjaer et al., 2012). SST data from Baffin Bay suggest that ocean warming is a potential trigger for widespread glacier acceleration.

Thus there are two potential and opposite effects of increasing air temperature on iceberg occurrence between Greenland and the Grand Banks: more ice discharge from Greenland, and more iceberg deterioration due to reduced sea ice extent and higher ocean temperatures. However the latter effect appears to be dominant with respect to icebergs south of 48°N (Fig. 10).

8.0 CLIMATE INDICES

Much of the spatial variability in air temperature trends is due to changes in atmospheric circulation (Solomon et al., 2007), which is largely described by a few major patterns or indices. Indices of particular importance to North America are the North Atlantic Oscillation (NAO) index, the Pacific North American (PNA) index, and the East Pacific – North Pacific (EP-NP) index. The loading patterns of the indices and the correlation of the indices with surface temperature are shown by the NOAA National Weather Service Climate Prediction Center at <http://www.cpc.ncep.noaa.gov/data/teledoc/telecontents.shtml> (Appendix 4, Fig. A4-1), and the time series are plotted in Figure 12. In general terms, a positive winter NAO index is associated with a deepened Icelandic Low and low winter temperatures off the Canadian East Coast, while a positive PNA index is associated with a deepened Aleutian Low (Wallace and Gutzler, 1981) and high winter temperatures in western Canada. A positive winter NAO index is also associated with longer durations of river and lake ice in eastern Canada, and a positive PNA index is associated with shorter durations of river and lake ice in western Canada (Prowse et al., 2011).

The NAO is closely related to the Arctic Oscillation (AO), also referred to as the Northern Annular Mode (NAM), and the two time series are highly correlated in winter (Solomon et al., 2007). The PNA index, which only extends back to about 1950, is highly anti-correlated with the North Pacific Index (Fig. 12; Trenberth and Hurrell, 1994) which extends back to 1899. The NP index is defined as the area-weighted SLP over the region 30-65°N, 160-140°W.

Another Pacific mode, the East Pacific – North Pacific (EP-NP) index (Barnston and Livezey, 1987), is important in spring, summer and autumn. A positive autumn EP-NP index is associated with high (low) pressure anomalies over western (eastern) Canada, and low temperatures in eastern Canada. In particular, Hochheim et al. (2010) found autumn surface air temperature in the Hudson Bay region was highly anti-correlated with

the EP-NP index, and that a low EP-NP index since the mid-1990s has resulted in reduced sea ice during the freeze-up period.

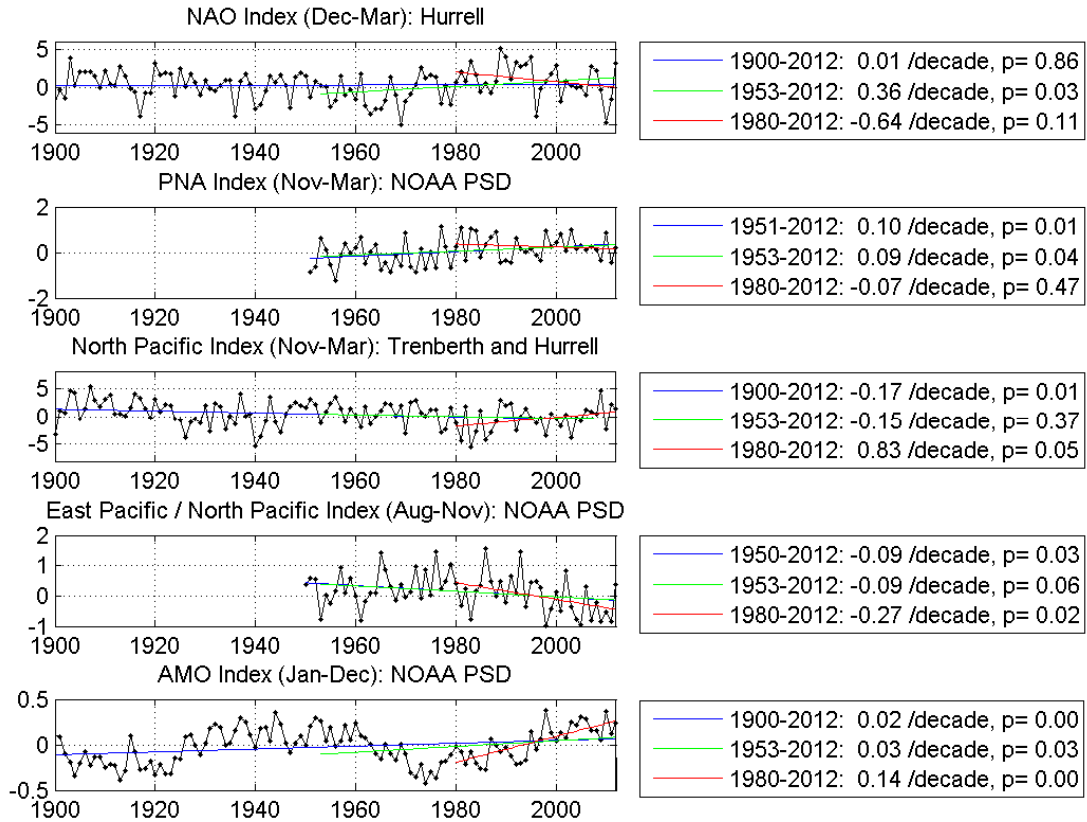


Fig. 12. Anomalies of North Atlantic Oscillation (NAO), Pacific North American (PNA), North Pacific (NP), East Pacific – North Pacific (EP-NP) and Atlantic Multidecadal Oscillation (AMO) indices (1900-2012).

Figure 12 also shows the Atlantic Multidecadal Oscillation (AMO), representing the detrended mean sea surface temperature in the North Atlantic south of 70°N (Enfield et al., 2001, <http://www.esrl.noaa.gov/psd/data/timeseries/AMO/>). The AMO has a period of 65-80 years (Enfield et al., 2001), with warm phases in about 1925-1965 and since 1995, and cool phases in 1901-1924 and 1966-1994 (Fig. 12, Wang et al., 2008). Regression coefficients associated with surface temperature regressed on the AMO are highest in the Atlantic subpolar gyre area and over eastern Canada (Fig. A4-2, Knight et al., 2005). For the North Atlantic region, the first EOF of SST from various datasets closely

resembles the AMO (Loder et al., 2013). The AMO is anti-correlated with SLP centred at about 22°N, in the southern part of the subtropical anticyclone (Fig. A4-2); a similar correlation pattern between detrended mean sub-tropical SST and geopotential height was shown by Walter and Graf (2002). The spatial pattern of surface air temperature associated with the AMO (Fig. A4-2) is consistent with the SLP pattern.

There is some evidence of 55-100 year oscillations in paleoclimate records of North Atlantic ocean-atmosphere variability over the past 500 to 8,000 years (Gray et al., 2004; Knudsen et al., 2011). Although the forcing mechanisms of the AMO are not well understood, the AMO appears to be related to the NAO, with the AMO lagging the multidecadal NAO signal by about a decade (Delworth and Mann; 2000; Latif et al. 2006). Model simulations suggest that a high NAO anomaly increases the AMOC by enhancing the subpolar gyre and North Atlantic Current, thereby enhancing the advection of warm, salty water into the deep convection regions (Dong and Sutton, 2005), and by increasing Labrador Sea convection (Latif et al., 2006). An increase in the AMOC produces warm SST anomalies in the subpolar gyre and a meridional SST gradient. The SST gradient results in a weakening of the North Atlantic Hadley cell and northeasterly trade winds, a northward shift of the ITCZ, and a strengthening of northward oceanic heat transport ((Mantsis and Clement, 2009; Smith et al., 2010). Thus model simulations suggest that the atmosphere drives SST anomalies associated with the AMO in high latitudes, but these SST anomalies drive atmospheric anomalies in low latitudes.

Hakkinen et al. (2011) have also suggested that high frequency of atmospheric blocking events in winter between Greenland and western Europe corresponds to warmer, more saline subpolar waters, and the warm phase of the AMO or AMV (Atlantic Multidecadal Variability). The wind forcing associated with the blocking may result in weaker ocean gyres and weaker heat exchange, contributing to the warm phase of the AMO.

Multidecadal SST variability may also be caused by multidecadal fluctuations of net shortwave radiation linked to aerosol and volcanic changes, either as a direct response to changes in solar forcing, or through some interaction with internal modes of the coupled

system. Ottera et al. (2010) showed that the phasing of multidecadal variability in North Atlantic SST over the past 150 years can be accounted for by variations in volcanic activity, but not the amplitude. In another model study, Booth et al (2012) showed that aerosol emissions and volcanic activity explain most of the variability in Atlantic SST since 1860. However major discrepancies were found between simulations by their model and observations of several other key variables, casting some doubt on the claim that aerosol forcing drives the bulk of multidecadal SST variability (Zhang et al., 2013).

8.1 AIR TEMPERATURE

Correlations between seasonal air temperature at the 17 stations (Appendix 1) and the climatic indices (Fig. 12) for the period 1950-2012 are shown in Table 2. The correlation coefficients for the AMO generally range from 0.2 to 0.6, with lower values in the winter and at Churchill. Correlations for the NAO in winter are generally significant in Labrador, Nunavut, Greenland, and eastern Hudson Bay, with values of -0.5 to -0.7. In spring, correlations for the NAO are weaker than in winter. For the PNA in winter, a significant correlation is found only at Churchill, of the 17 stations, in agreement with the correlation map in Fig. A4-1. The EP-NP index shows a significant relationship with air temperature at many stations in Hudson Bay and the Gulf of St. Lawrence in summer and autumn.

Trends for the time series of the NAO (Hurrell, 1995), PNA, NP (Trenberth and Hurrell, 1994), EP-NP, and AMO indices are listed in Figure 12. For the period 1900-2012, the trend for the NAO is not significant ($p > 0.05$). However, there is a significant negative trend for the NP index. This is consistent with higher temperature trends west of Hudson Bay and lower trends in southern Greenland (Fig. 1: Fig 3-9, Solomon et al., 2007).

For the period 1953-2012, there is a positive significant trend for both the NAO and PNA indices, which is consistent with higher annual, winter and spring air temperature trends in western Canada than eastern Canada during this period (Zhang et al., 2011). Most of the temperature trends are significant in summer and autumn, but few are significant in winter and spring (Appendix 1). A positive trend for the AMO would result in positive air

temperature trends throughout the year. However in winter and spring, temperature variability is dominated by decadal variations associated with the NAO, so that fewer of the trends are significant.

Table 2. Correlations (r) of seasonal air temperature with climatic indices for the 1950-2012 period. An asterisk indicates the correlation is significant at the 5% level (with no correction for autocorrelation).

	Winter (DJF)			Spring (MAM)		Summer (JJA)		Autumn (SON)	
	NAO (DJF)	PNA (DJF)	AMO (DJF)	NAO (MAM)	AMO (MAM)	EP-NP (JJA)	AMO (JJA)	EP-NP (ASON)	AMO (ASON)
Upernavik	-0.58*	-0.11	0.26	-0.26	0.07	0.19	0.40*	-0.07	0.32*
Nuuk	-0.70*	-0.01	0.27*	-0.56*	0.41*	0.02	0.51*	-0.09	0.54*
Churchill	-0.16	0.51*	0.23	-0.28*	0.16	-0.56*	0.32*	-0.67*	0.27*
Cape Dorset	-0.54*	-0.06	0.28*	-0.59*	0.53*	-0.29*	0.40*	-0.42*	0.57*
Iqaluit	-0.68*	0.03	0.33*	-0.58*	0.42*	-0.34*	0.42*	-0.37*	0.48*
Cartwright	-0.64*	0.04	0.43*	-0.49*	0.50*	-0.20	0.52*	-0.50*	0.63*
St. John's	-0.25	-0.01	0.48*	-0.09	0.25*	-0.07	0.34*	-0.48*	0.49*
Mont Joli	-0.24	0.11	0.60*	-0.22	0.42*	-0.31*	0.32*	-0.67*	0.55*
Charlottetown	-0.11	0.01	0.51*	-0.16	0.31*	-0.27*	0.26*	-0.63*	0.48*
Halifax	0.04	-0.00	0.37*	-0.24	0.36*	-0.30*	0.47*	-0.49*	0.42*
Aasiaat	-0.61*	0.01	0.36*	-0.35*	0.39*	0.01	0.64*	-0.12	0.53*
Resolute	-0.34*	0.24	0.28*	-0.42*	0.44*	-0.16	0.52*	-0.45*	0.49*
Clyde	-0.53*	0.04	0.26*	-0.39*	0.37*	-0.33*	0.54*	-0.32*	0.46*
Coral	-0.47*	0.17	0.25*	-0.55*	0.40*	-0.45*	0.38*	-0.55*	0.47*
Inukjuak	-0.41*	0.05	0.41*	-0.58*	0.49*	-0.53*	0.39*	-0.59*	0.38*
Kuujuarapik	-0.40*	0.13	0.54*	-0.52*	0.54*	-0.57*	0.40*	-0.73*	0.46*
Moosonee	-0.17	0.22	0.48*	-0.45*	0.42*	-0.48*	0.46*	-0.79*	0.41*

For the period 1980-2012, there is a negative (but not significant) trend for the NAO, and a small negative (but not significant) trend for the PNA index (Fig. 12), which is consistent with higher temperature trends for Greenland than west of Hudson Bay (Fig. 1, 3). The

trend for the AMO is higher in 1980-2012 than in 1953-2012 (Fig. 12), in agreement with air temperature trends which are higher and more significant for the 1980-2012 than the 1953-2012 period (Fig. 3).

8.2 SEA ICE

For the 1953-2011 period, winter sea ice variability is dominated by decadal variations associated with the NAO, so that few winter trends are significant (Table 1), and there is little difference in mean March ice coverage between 1961-1985 and 1986-2010 (Fig. 5). However summer sea ice in the Labrador Sea and Baffin Bay shows a nearly monotonic trend, so that trends are significant (Table 1), and mean July ice coverage in Baffin Bay decreases between 1961-1985 and 1986-2010 (Fig. 5). This is consistent with a study of sea ice variability in the northern hemisphere for the period 1958-1997 (Deser et al., 2000), based on the Chapman and Walsh (1993) dataset of gridded monthly mean sea ice concentrations. In general, winter sea ice variability was dominated by decadal variations associated with the North Atlantic Oscillation (NAO), but summer sea ice variability exhibited a nearly monotonic decline over that period.

In the study by Deser et al. (2000), it was found that the leading EOF in winter has a large amplitude in the Atlantic sector, with out-of phase variations between the Labrador and Greenland-Barents Sea, associated with the North Atlantic Oscillation (NAO), which is regarded as a subset of the spatially broader Arctic Oscillation (AO). Sea ice lagged SLP by 2-6 weeks. The trend in winter sea ice extent was -0.6% of the mean per decade, with strong decadal-scale variations. However regionally, sea ice extent showed a positive trend in the Labrador Sea for the 1958-1997 period, which offset negative trends elsewhere. Sea ice extent in summer showed a negative trend of -4% of the mean per decade, and was relatively monotonic. Arctic sea ice extent on shorter time scales (1979-2012) is declining faster, with trends of -2.6% per decade in March and -13.0% per decade in September (National Snow and Ice Data Center (NSIDC), <http://nsidc.org/>).

The decadal-scale variations in winter sea ice anomalies and associated SST anomalies for the Labrador Sea were described by Deser et al. (2002), with positive anomalies progressing from north to south over a 3-year period. Much of the winter-to-winter persistence could be attributed simply to atmospheric forcing, using a simple slab model. Mysak and Venegas (1998) described a feedback mechanism to account for the decadal cycle in sea ice concentration and SLP in the northern hemisphere. Decadal-scale variations also appeared to be present in records of ice severity in Hudson Bay and approaches for 1751-1870 based on from the Hudson's Bay Company ships' logbooks (Catchpole and Faurer, 1985), and in records of spring-summer sea ice in Davis Strait that drifted from east of Greenland (Defant, 1961).

For the 1980-2011 period, most trends in Table 1 are significantly different from zero, in agreement with Cavalieri and Parkinson (2012), Tivy et al. (2011a, 2011b), Henry (2011), and Hochheim and Barber (2010). During this period, the trend for the NAO is negative, the trend for the AMO is positive, and the trend for the EP-NP index is negative (Fig. 12), consistent with sea ice trends.

During the warm phase of the AMO in the 1920s and 1930s, low levels of sea ice were observed off southwest Greenland. Storis (i.e. sea ice from the Arctic Ocean drifting northward along the southwestern Greenland coast from Cape Farewell), generally reaches its northernmost position in May. The northernmost position of storis was particularly low at this time (Drinkwater, 2006; Schmith and Hansen, 2003).

9.0 CONCLUSIONS

For the 1900-2012 period, annual mean air temperature trends in eastern Canada south of 50°N were 0.05-0.16 °C/decade and significant at the 5% level at all 4 stations examined, and were comparable to the global mean of 0.074 °C/decade for the period 1906-2005 (Solomon et al., 2007). In southwestern Greenland, annual air temperature trends were not significant ($p>0.05$) at 2 of the 3 stations examined, and the trend at Nuuk was only 0.03 °C/decade. Greenland temperature trends were highest and

significant in winter, and lowest and not significant in spring, in agreement with Box (2002).

For the 1953-2012 period, annual mean air temperature trends along the Canadian East Coast south of 50°N were 0.13-0.22 °C/decade and significant at the 5% level, and were comparable to the global mean of 0.13°C/decade for the period 1956-2005 (Solomon et al., 2007). Overall, most of the annual trends were significant except in southwestern Greenland and near Hudson Strait. In winter, most of the trends were not significant ($p > 0.05$) and relatively low, while in summer and autumn, most of the trends were significant ($p < 0.05$) and relatively high. In comparison, most of the annual ice area trends were not significant for the 1953-2012 period. In winter and autumn, most of the ice area trends were not significant and relatively weak, while in summer, most of the trends were significant ($p < 0.05$) and relatively strong. Thus the air temperature and ice area trends are consistent for winter and summer. The contrast between winter and summer trends is in agreement with Deser et al. (2000), and can be attributed to high decadal variability in winter associated with the NAO.

For the 1980-2012 period, annual mean air temperature trends in eastern Canada south of 50°N were 0.29-0.56 °C/decade and significant at the 5% level, and were higher than the global mean of 0.18°C/decade for the period 1981-2005 (Solomon et al., 2007). Trends were even higher north of 50°N, with values of 0.8-0.9 °C/decade in Canada, and 0.8-1.3 °C/decade in Greenland. Overall, all except one of the annual trends were significant. Most of the seasonal trends were significant ($p < 0.05$), except in spring, when few of the trends in eastern Canada south of 65°N were significant. In comparison, all of the annual ice area trends were significant ($p < 0.05$) for the 1980-2012 period. For all seasons, most of the ice area trends were significant, except for Hudson Bay and Hudson Strait in winter, when these areas are almost completely ice-covered. The high air temperature trends in 1980-2012 can be attributed in part to the negative NAO trend and positive AMO trend.

10.0 ACKNOWLEDGMENTS

We wish to thank John Loder, Jim Hamilton and Daniel Caissie for reviewing the manuscript. This study was funded in part by the Aquatic Climate Change Adaptation Services Program of Fisheries and Oceans Canada. NCEP Reanalysis data provided by the NOAA/OAR/ESRL PSD, Boulder, Colorado, USA, from their Web site at <http://www.esrl.noaa.gov/psd/>

11.0 REFERENCES

- Anderson, I. 1993. International Ice Patrol Iceberg Sighting Data Base 1960-1991, Appendix D in Report of the International Ice Patrol in the North Atlantic, Bulletin No. 79, 1993 Season, CG-188-48, Washington, DC.
- Barnston, A.G., and R.E. Livezey, 1987. Classification, seasonality and persistence of low-frequency atmospheric circulation patterns. *Mon. Wea. Rev.*, **115**, 1083-1126.
- Booth, B.B.B., N.J. Dunstone, P.R. Halloran, T. Andrews, and N. Bellouin. 2012. Aerosols implicated as a prime driver of twentieth-century North Atlantic climate variability. *Nature*, 484, 228–232.
- Box, J.E. 2002. Survey of Greenland instrumental temperature records: 1873-2001, *International Journal of Climatology*, 22, 1829-1847.
- Cavalieri, D.J., and C.L. Parkinson. 2012. Arctic sea ice variability and trends, 1979-2010 *The Cryosphere*, 6, 881-889 10.5194/tc-6-881-2012
- Catchpole, A.J.W. and M.A. Faurer. 1985. Ships' Log-Books, Sea Ice and the Cold Summer of 1816 in Hudson Bay and Its Approaches, *Arctic* 38(2):121-128.
- Chapman, W.L., and J.E. Walsh. 1993. Recent variations of sea ice and air temperature in high latitudes. *Bull. Amer. Meteor. Soc.*, 74, 33–47.
- Colbourne, E., J. Craig, C. Fitzpatrick, D. Senciall, P. Stead and W. Bailey. 2011. An assessment of the physical oceanographic environment on the Newfoundland and Labrador Shelf during 2010. DFO Can. Sci. Advis. Sec. Res. Doc. 2011/089. iv + 31p.
- Crane, R.G. 1978. Seasonal variations of sea ice extent in the Davis Strait-Labrador Sea area and relationships with synoptic-scale atmospheric circulation. *Arctic*, 31, 434–447.
- Defant, A. 1961. *Physical Oceanography*, Vol. 1. Macmillan, 728 pp.

Delworth, T.L. and M.E. Mann. 2000. "Observed and simulated multidecadal variability in the Northern Hemisphere". *Climate Dynamics* **16**: 661–676. doi:10.1007/s003820000075

Deser, C., J.E. Walsh, and M.S. Timlin. 2000. Arctic sea ice variability in the context of recent wintertime atmospheric circulation trends. *Journal of Climate*, **13**, 617–633.

Deser, C., M. Holland, G. Reverdin, and M.S. Timlin. 2002. Decadal variations in Labrador Sea ice cover and North Atlantic sea surface temperatures. *Journal of Geophysical Research-Oceans*, **107**, 10.1029/2000JC000683.

Dong, B. and T.R. Sutton. 2005. Mechanism of Interdecadal Thermohaline Circulation Variability in a Coupled Ocean–Atmosphere GCM. *J. Climate*, **18**, 1117–1135. doi: <http://dx.doi.org/10.1175/JCLI3328.1>

Drijfhout, S., G.J. van Oldenborgh and A. Cimadoribus. 2012. Is a Decline of AMOC Causing the Warming Hole above the North Atlantic in Observed and Modeled Warming Patterns?. *J. Climate*, **25**, 8373–8379.

Drinkwater, K.F. 2006. The regime shift of the 1920s and 1930s in the North Atlantic. *Progress in Oceanography* **68**, 134–151.

Dumas, J.A., G.M. Flato, and R.D. Brown. 2006. Future Projections of Landfast Ice Thickness and Duration in the Canadian Arctic. *J. Climate*, **19**, 5175–5189. doi: <http://dx.doi.org/10.1175/JCLI3889.1>

Enfield, D.B., A.M. Mestas-Nunez, and P.J. Trimble. 2001. The Atlantic Multidecadal Oscillation and its relationship to rainfall and river flows in the continental U.S., *Geophys. Res. Lett.*, **28**: 2077-2080.

Galbraith, P.S., and P. Larouche. P. 2011. Sea-surface temperature in Hudson Bay and Hudson Strait in relation to air temperature and ice cover breakup, 1985-2009: *Journal of Marine Systems*, v. **87**, no. **1**, p. 66-78.

Galbraith, P.S., J. Chassé, D. Gilbert, P. Larouche, D. Brickman, B. Pettigrew, L. Devine, A. Gosselin, R. G. Pettipas and C. Lafleur. 2011. Physical Oceanographic Conditions in the Gulf of St. Lawrence in 2010. DFO Can. Sci. Advis. Sec. Res. Doc. 2011/045. iv + 82 p.

Gray, S. T., L.J. Graumlich, J.L. Betancourt, and G.T. Pederson. 2004. A tree-ring based reconstruction of the Atlantic Multidecadal Oscillation since 1567 A.D., *Geophys. Res. Lett.*, **31**, L12205, doi:10.1029/2004GL019932.

Hakkinen, S., P.B. Rhines and D.L. Worthen. 2011. Atmospheric Blocking and Atlantic Multidecadal Ocean Variability *Science*, **334**(6056), 655-659 10.1126/science.1205683

Hebert, D., R. Pettipas and B. Petrie. 2011. Meteorological, Sea Ice and Physical Oceanographic Conditions on the Scotian Shelf and in the Gulf of Maine during 2009 and 2010 DFO Can. Sci. Advis. Sec. Res. Doc. 2011/094. v + 32 p

Henry, M. 2011. Sea ice trends in Canada, Statistics Canada Envirostats Bulletin Vol. 5(4), Catalogue no. 16-002-X.

Hill, B. 1999. Historical Record of sea ice and iceberg distribution around Nfld and Labrador, 1810-1958 WCRP No. 108 or WMO/TD No. 949, April/99, ACSYS, Proc. of the Workshop on Sea Ice Charts of the Arctic, Seattle, WA AU 5-7, 1998.

Hochheim, K.P. and D. G. Barber. 2010. Atmospheric forcing of sea ice in Hudson Bay during the fall period, 1980–2005, *J. Geophys. Res.*, 115, C05009, doi:10.1029/2009JC005334.

Holland, D M., R.H. Thomas, B. de Young, M.H. Ribergaard and B. Lyberth. 2008. Acceleration of Jakobshavn Isbrae triggered by warm ocean waters. *Nature Geoscience* 1 (10): 659–664. doi:10.1038/ngeo316

Hurrell, J.W. 1995. Decadal Trends in the North Atlantic Oscillation: Regional Temperatures and Precipitation. *Science*: Vol. 269, pp.676-679

IPCC, 2007. Summary for Policymakers. In: *Climate Change 2007: The Physical Science Basis. Contribution of Working Group I to the Fourth Assessment Report of the Intergovernmental Panel on Climate Change* [Solomon, S., D. Qin, M. Manning, Z. Chen, M. Marquis, K.B. Averyt, M.Tignor and H.L. Miller (eds.)]. Cambridge University Press, Cambridge, United Kingdom and New York, NY, USA.

Kalnay, E., M. Kanamitsu, R. Kistler, W. Collins, D. Deaven, L. Gandin, M. Iredell, S. Saha, G. White, J. Woollen, Y. Zhu, M. Chelliah, W. Ebisuzaki, W.Higgins, J. Janowiak, K.C. Mo, C. Ropelewski, J. Wang, A. Leetmaa, R. Reynolds, R. Jenne and D. Joseph. 1996. The NCEP/NCAR 40-Year Reanalysis Project. *Bulletin of the American Meteorological Society* 77 (3): 437–471.

Kjær, K.H., S.A. Khan, N.J. Korsgaard, J. Wahr, J.L. Bamber, R. Hurkmans, M. van den Broeke, L.H. Timm, K.K. Kjeldsen, A.A. Bjørk, N.K. Larsen, L.T. Jørgensen, A. Færch-Jensen and E. Willerslev. 2012. Aerial Photographs Reveal Late–20th-Century Dynamic Ice Loss in Northwestern Greenland *Science* 3 August 2012: 337 (6094), 569-573. DOI:10.1126/science.1220614

Knight, J.R., R.J. Allan, C.K. Folland, M. Vellinga, and M.E. Mann. 2005. A signature of persistent natural thermohaline circulation cycles in observed climate, *Geophys. Res. Lett.*, 32, L20708, doi:10.1029/2005GL024233

Knudsen, M.F., M.S. Seidenkrantz, B.H. Jacobsen, and A. Kuijpers. 2011. Tracking the Atlantic Multidecadal Oscillation through the last 8,000 years. *Nature*

Communications, 2, 178.

Latif, M., C. Böning, J. Willebrand, A. Biastoch, J. Dengg, N. Keenlyside, U. Schweckendiek and G. Madec, 2006: Is the Thermohaline Circulation Changing?. *J. Climate*, **19**, 4631–4637. doi: <http://dx.doi.org/10.1175/JCLI3876.1>

Loder, J.W., Z. Wang, A. van der Baaren and R. Pettipas, 2013. Trends and variability of sea surface temperature (SST) in the Northwest Atlantic, from the HadISST, ERSST and COBE datasets. *In: Aspects of climate change in the NW Atlantic off Canada*. [Loder, J.W., A. van der Baaren and G. Han (Eds.)], Can Tech. Rep. Fish. Aquat. Sci. 3045.

Mantsis, D.F., and A.C. Clement. 2009, Simulated variability in the mean atmospheric meridional circulation over the 20th century, *Geophys. Res. Lett.*, 36, L06704, doi:10.1029/2008GL036741.

Markus, T., J.C. Stroeve, and J. Miller. 2009. Recent changes in Arctic sea ice melt onset, freezeup, and melt season length, *J. Geophys. Res.*, 114, C12024, doi:10.1029/2009JC005436.

Meehl, G.A., T.F. Stocker, W.D. Collins, P. Friedlingstein, A.T. Gaye, J.M. Gregory, A. Kitoh, R. Knutti, J.M. Murphy, A. Noda, S.C.B. Raper, I.G. Watterson, A.J. Weaver and Z.-C. Zhao, 2007: Global Climate Projections. *In: Climate Change 2007: The Physical Science Basis. Contribution of Working Group I to the Fourth Assessment Report of the Intergovernmental Panel on Climate Change* [Solomon, S., D. Qin, M. Manning, Z. Chen, M. Marquis, K.B. Averyt, M. Tignor and H.L. Miller (eds.)]. Cambridge University Press, Cambridge, United Kingdom and New York, NY, USA.

Mysak, L.A. and S.A. Venegas. 1998. Decadal climate oscillations in the Arctic: A new feedback loop for atmosphere–ice–ocean interactions, *Geophys. Res. Lett.*, 25(19), 3607–3610, doi:10.1029/98GL02782.

Ottera°, O.H., M. Bentsen, H. Drange and L. Suo. 2010. External forcing as a metronome for Atlantic multidecadal variability. *Nat. Geosci.* 3, 688–694.

Peterson, I.K. 2004. Long-Range Forecasting of the Iceberg Population on the Grand Banks, *In Proceedings of the Fourteenth (2004) International Offshore and Polar Engineering Conference Toulon, France, May 23-28, 2004, Vol. I*, pp. 831-836

Peterson, I.K., S.J. Prinsenberg and J.S. Holladay. 2003. Sea-ice thickness measurement: Recent experiments using helicopter-borne electromagnetic systems, *Recent Res. Devel. Geophysics* 5(2003): 1-20.

Peterson, I.K., S.J. Prinsenberg, and P. Langille. 2000. Sea Ice Fluctuations in the Western Labrador Sea (1963-1998). *Can. Tech. Rep. Hydrogr. Ocean Sci.* 208: v+51 p.

Peterson, I.K., S.J. Prinsenberg and D. Belliveau. 2013. Sea Ice Draft and Velocities from Moorings on the Labrador Shelf (Makkovik Bank): 2003-2011. Can. Tech. Rep. Hydrogr. Ocean Sci. 281: v + 32 p.

Prinsenberg, S.J., I.K. Peterson, S. Narayanan, S. and J.U.Umoh. 1997. Interaction between Atmosphere, Ice Cover and Ocean off Labrador and Newfoundland from 1962 to 1992. Can. J. Fish. Aquat. Sci. 54(Suppl. 1):30-39.

Prinsenberg, S.J., I.K. Peterson, J.S. Holladay and L. Lalumiere, 2012. Labrador Shelf Pack Ice and Iceberg Survey, March 2011. Can. Tech. Rep. Hydrogr. Ocean Sci. 275: vii+44pp.

Prowse, T., K. Alfredsen, S. Beltaos, B. Bonsal, C. Duguay, A. Korhola, J. McNamara, R. Pienitz, W.F. Vincent, V. Vuglinsky and G.A. Weyhenmeyer 2011. Past and future changes in Arctic lake and river ice. *Ambio* 40:53–62. DOI 10.1007/s13280-011-0216-7

Rayner, N.A., Parker, D.E., Horton, E.B., Folland, C.K., Alexander, L.V., Rowell, D.P., Kent, E.C. and A. Kaplan. 2003. Global analyses of sea surface temperature, sea ice, and night marine air temperature since the late nineteenth century, *J. Geophys. Res.*, Vol. 108, No. D14, 4407 10.1029/2002JD002670

Rignot, E. and P. Kanagaratnam. 2006. Changes in the velocity structure of the Greenland Ice Sheet. *Science*, 311(5763), 956-990, doi:10.1126/science.1121381

Rignot, E., I. Velicogna and M.R. van den Broeke, A. Monaghan, and J. Lenaerts. 2011. Acceleration of the contribution of the Greenland and Antarctic ice sheets to sea level rise, *Geophys. Res. Lett.*, 38, L05503, doi:10.1029/ 2011GL046583.

Schmith, T. and C. Hansen. 2003. Fram Strait ice export during the nineteenth and twentieth centuries reconstructed from a multiyear sea ice index from southwestern Greenland. *J. Climate*, 16, 2782–2791.

Serreze, M.C. and R.G. Barry. 2011. Processes and impacts of Arctic amplification: A research synthesis. *Glob. Planet. Change*, 77 (2-Jan) 85-96, issn: 0921-8181, ids: 787ET, doi: 10.1016/j.gloplacha.2011.03.004

Smith, D.M., R. Eade, N.J. Dunstone, D. Fereday, J.M. Murphy, H. Pohlmann, A. Scaife, 2010. Skilful multi-year predictions of Atlantic hurricane frequency. *Nat. Geosci.*, 3, 846-849. doi:10.1038/ngeo1004

Smith, E.H. 1931. The Marion Expedition to Davis Strait and Baffin Bay, 1928. U.S. Coast Guard Bull. No. 19, Part 3, 221 p.

Solomon, S., D. Qin, M. Manning, R.B. Alley, T. Berntsen, N.L. Bindoff, Z. Chen, A. Chidthaisong, J.M. Gregory, G.C. Hegerl, M. Heimann, B. Hewitson, B.J. Hoskins, F. Joos, J. Jouzel, V. Kattsov, U. Lohmann, T. Matsuno, M. Molina, N. Nicholls, J.

Overpeck, G. Raga, V. Ramaswamy, J. Ren, M. Rusticucci, R. Somerville, T.F. Stocker, P. Whetton, R.A. Wood and D. Wratt. 2007. Technical Summary. In: *Climate Change 2007: The Physical Science Basis. Contribution of Working Group I to the Fourth Assessment Report of the Intergovernmental Panel on Climate Change* [Solomon, S., D. Qin, M. Manning, Z. Chen, M. Marquis, K.B. Averyt, M. Tignor and H.L. Miller (eds.)]. Cambridge University Press, Cambridge, United Kingdom and New York, NY, USA.

Thistle, M.E. and D. Caissie. 2013. Trends in air temperature, total precipitation, and streamflow characteristics in eastern Canada. *Can. Tech. Rep. Fish. Aquat. Sci.* 3018: xi + 97p.

Tivy, A., S.E.L. Howell, B. Alt, S. McCourt, R. Chagnon, G. Crocker, T. Carrieres, and J. Yackel. 2011a. Trends and variability in summer sea ice cover in the Canadian Arctic based on the Canadian Ice Service Digital Archive, 1960–2008 and 1968–2008, *J. Geophys. Res.*, 116, C03007, doi:10.1029/2009JC005855.

Tivy, A., S.E.L. Howell, B. Alt, S. McCourt, R. Chagnon, G. Crocker, T. Carrieres, and J. Yackel. 2011b. Correction to “Trends and variability in summer sea ice cover in the Canadian Arctic based on the Canadian Ice Service Digital Archive, 1960–2008 and 1968–2008,” *J. Geophys. Res.*, 116, C06027, doi:10.1029/2011JC007248.

Trenberth, K.E. and J.W. Hurrell. 1994. Decadal atmosphere-ocean variations in the Pacific, *Climate Dynamics* 9:303-319.

Våge, K., R.S. Pickart, V. Thierry, G. Reverdin, C.M. Lee, B. Petrie, T.A. Agnew, A. Wong, and M.H. Ribergaard. 2009. Surprising return of deep convection to the subpolar North Atlantic Ocean in winter. *Nature Geoscience*. 2, January 2009, 67-72. Published online (www.nature.com/naturegeoscience): 30 November 2008 doi: 10.1038/NGEO382.

Vincent, L.A., E.J. Milewska, R. Hopkinson and L. Malone. 2009. Bias in minimum temperature introduced by a redefinition of the climatological day at the Canadian synoptic stations. *Journal of Applied Meteorology and Climatology*, 48, 2160-2168. DOI: 10.1175/2009JAMC2191.1.

Vincent, L.A., X.L. Wang, E.J. Milewska, H. Wan, F. Yang, and V. Swail. 2012. A second generation of homogenized Canadian monthly surface air temperature for climate trend analysis, *J. Geophys. Res.*, 117, D18110, doi:10.1029/2012JD017859.

Wadhams, P., A.S. McLaren, and R. Weintraub. 1985. Ice thickness distribution in Davis Strait in February from submarine sonar profiles, *J. Geophys. Res.*, 90(C1), 1069–1077, doi:10.1029/JC090iC01p01069

Wallace, J.M. and D.S. Gutzler. 1981. Teleconnections in the Geopotential Height Field during the Northern Hemisphere Winter. *Mon. Wea. Rev.*, 109, 784–812.

Walsh, J.E. 1978. A data set on Northern Hemisphere sea ice extent, 1953– 76, *Glaciol. Data Rep. GD-2, Arctic Sea Ice, Part 1*, pp. 49 – 51, <http://nsidc.org/>, World Data Cent. for Glaciol., Boulder, Colo.

Walsh, J.E. and C.M. Johnson. 1979. Interannual atmospheric variability and associated fluctuations in Arctic Sea ice extent, *J. Geophys. Res.*, 84(C11), 6915–6928, doi:10.1029/JC084iC11p06915.

Walter, K. and H.-F. Graf. 2002. On the changing nature of the regional connection between the North Atlantic Oscillation and sea surface temperature, *J. Geophys. Res.*, 107(D17), 4338, doi:10.1029/2001JD000850.

Wang, C., S.-K. Lee, and D.B. Enfield. 2008. Atlantic Warm Pool acting as a link between Atlantic Multidecadal Oscillation and Atlantic tropical cyclone activity, *Geochem. Geophys. Geosyst.*, 9, Q05V03, doi:10.1029/2007GC001809.

Woollings, T., J.M. Gregory, J.G. Pinto, M. Reyers, and D.J. Brayshaw. 2012a. Response of the North Atlantic storm track to climate change shaped by ocean-atmosphere coupling, *Nat. Geosci.*, 5, 313–317.

Woollings, T., B. Harvey, M. Zahn, and L. Shaffrey. 2012b. On the role of the ocean in projected atmospheric stability changes in the Atlantic polar low region, *Geophys. Res. Lett.*, 39, L24802, doi:10.1029/2012GL054016.

Wu, Y., C.G. Hannah, B. Petrie, R. Pettipas, I. Peterson, S. Prinsenberg, C. Lee and D. Moritz. 2013. Ocean current and sea ice statistics for Davis Strait. *Can. Tech. Rep. Hydrogr. Ocean Sci.* 284: vi + 47p.

Zhang, R., T.L. Delworth, R. Sutton, D. L.R. Hodson, K.W. Dixon, I.M. Held, Y. Kushnir, J. Marshall, Y. Ming, R. Msadek, J. Robson, A.J. Rosati, M. Ting and G.A. Vecchi. 2013: Have Aerosols Caused the Observed Atlantic Multidecadal Variability?. *J. Atmos. Sci.*, **70**, 1135–1144. doi: <http://dx.doi.org/10.1175/JAS-D-12-0331.1>

Zhang, X., R. Brown, L. Vincent, W. Skinner, Y. Feng and E. Mekis. 2011. Canadian climate trends, 1950-2007. *Canadian Biodiversity: Ecosystem Status and Trends 2010*, Technical Thematic Report No. 5. Canadian Councils of Resource Ministers. Ottawa, ON. iv + 21 p. <http://www.biodivcanada.ca/default.asp?lang=En&n=137E1147-0>

APPENDIX 1. SEASONAL AIR TEMPERATURE TIME SERIES.

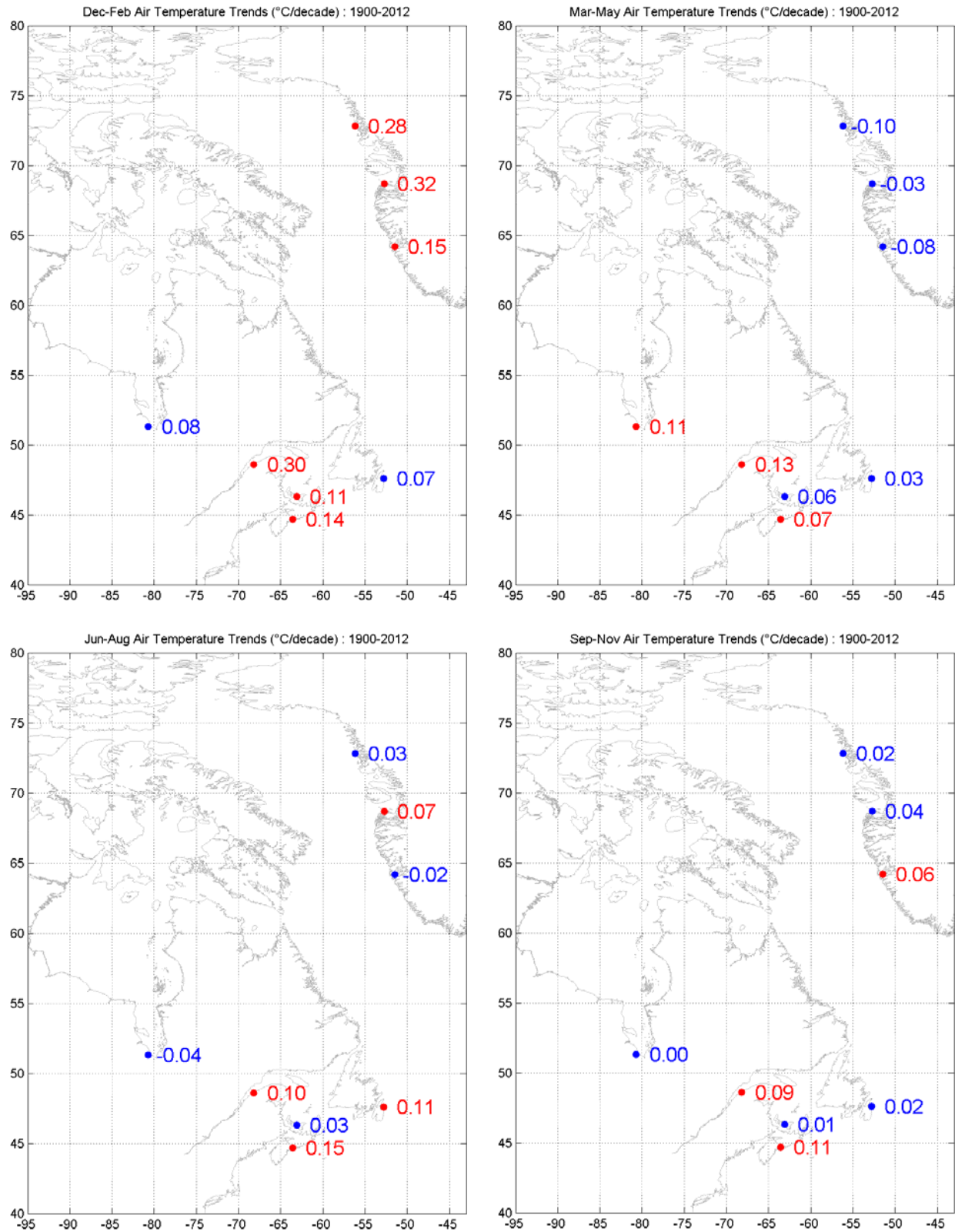


Fig. A1-1. Seasonal air temperature trends, 1900-2012 : red indicates $p < 0.05$.

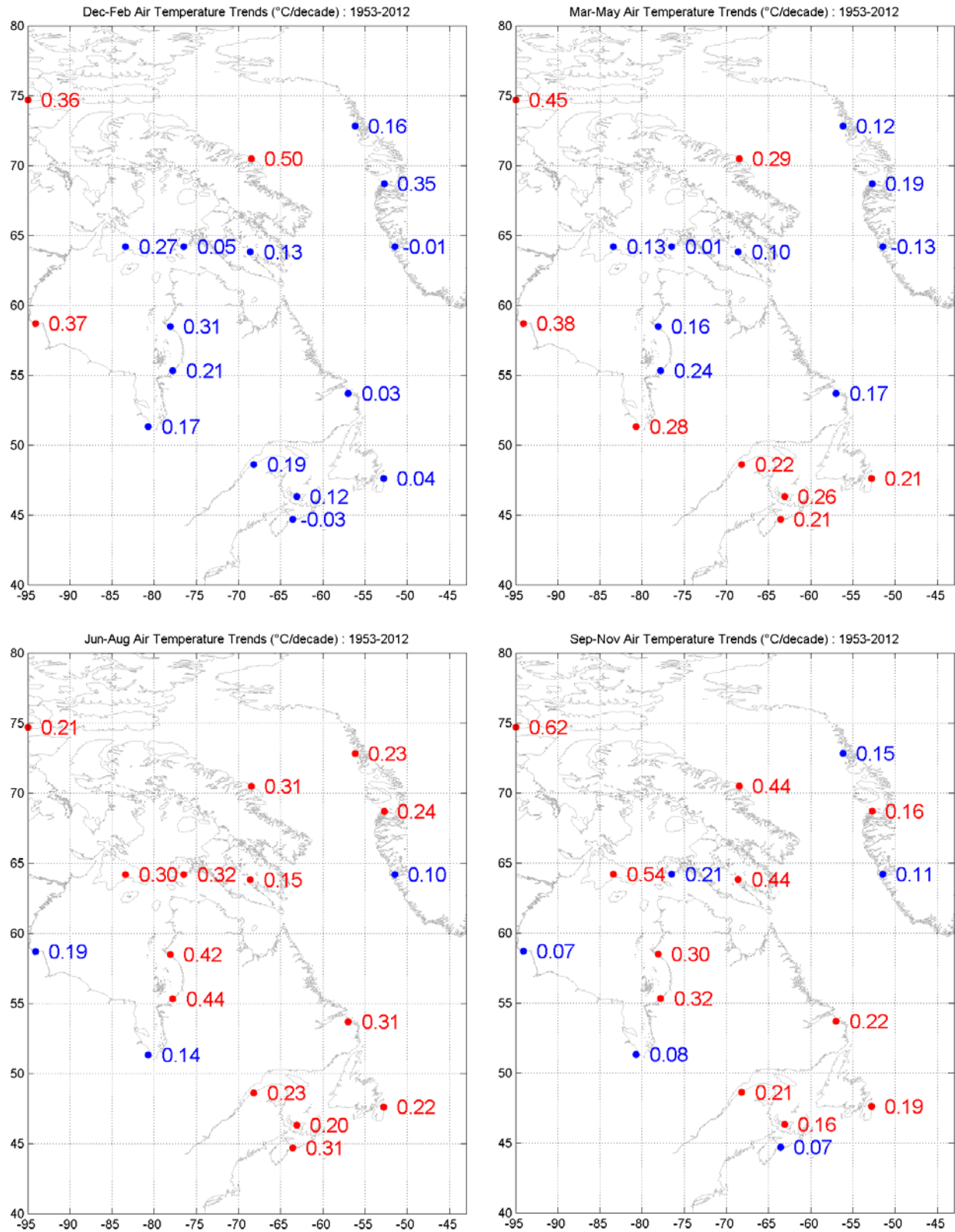


Fig. A1-2. Seasonal air temperature trends, 1953-2012 : red indicates $p < 0.05$.

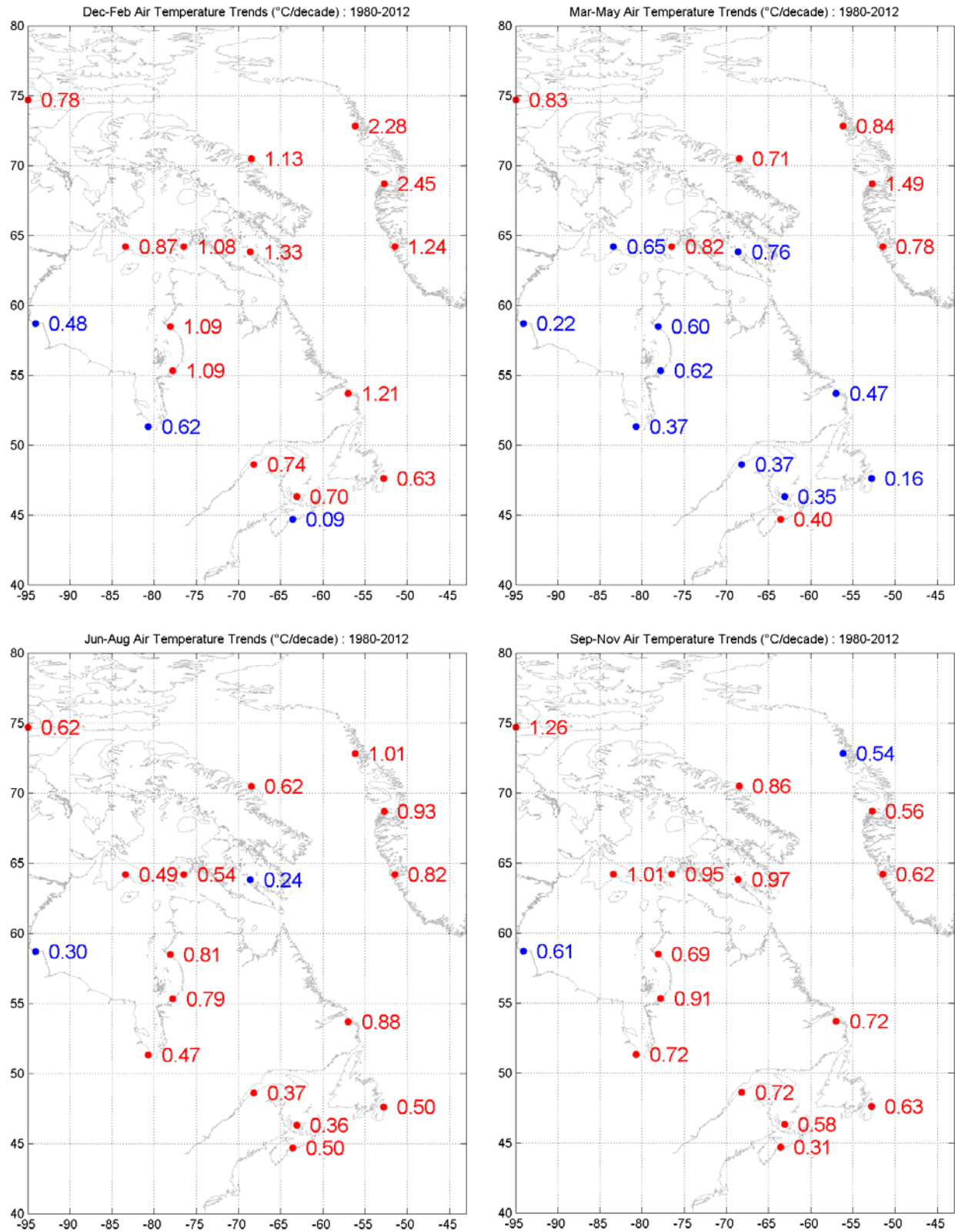


Fig. A1-3. Seasonal air temperature trends, 1980-2012 : red indicates $p < 0.05$.

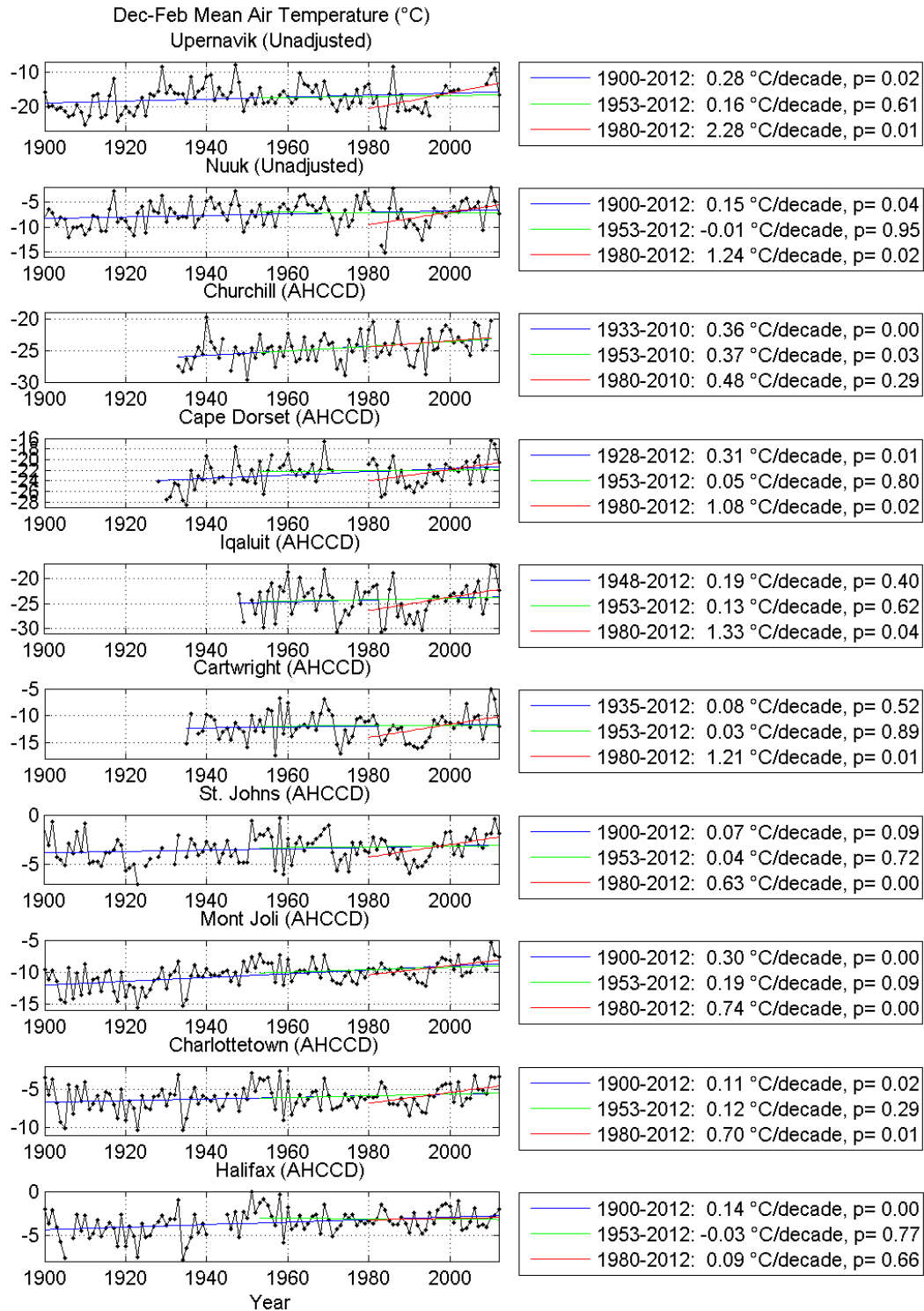


Fig. A1-4. Winter (Dec-Feb) mean air temperatures.

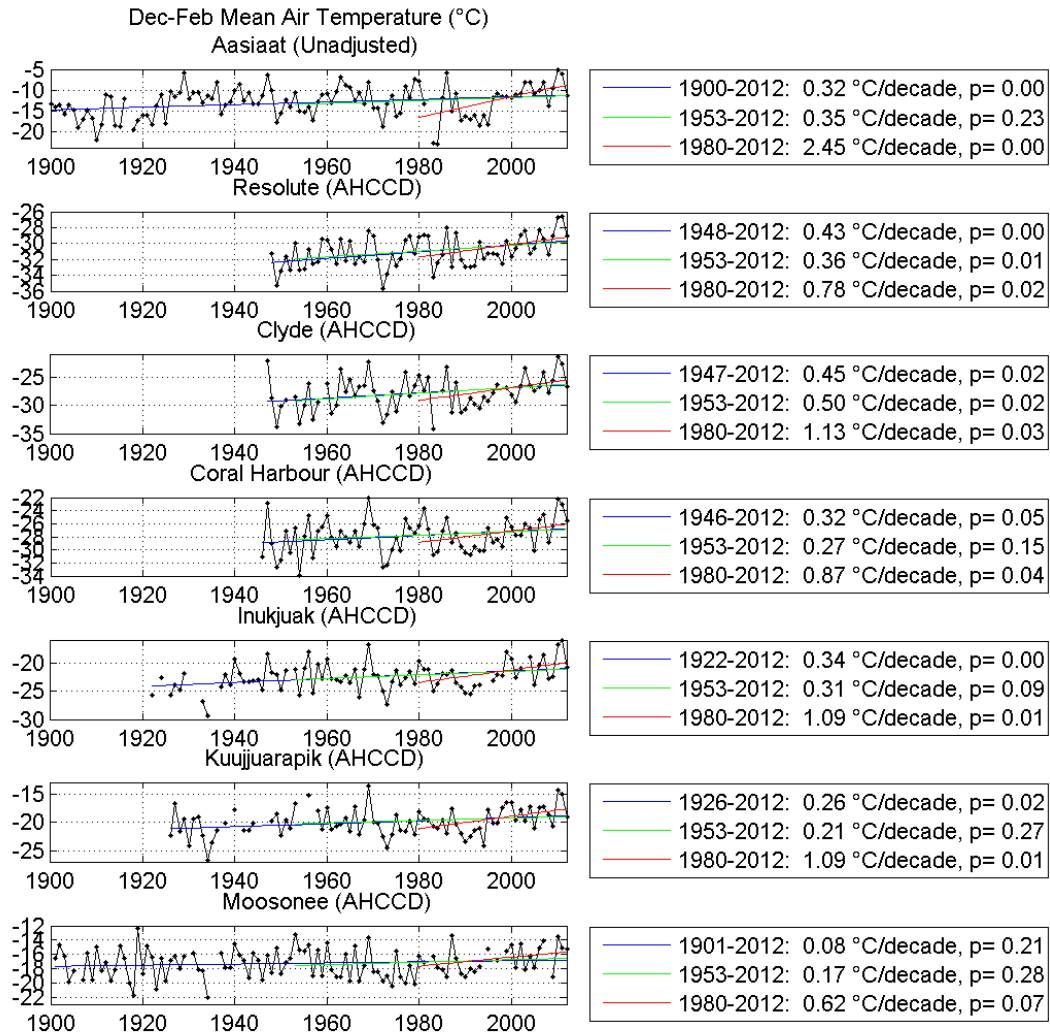


Fig. A1-4. continued.

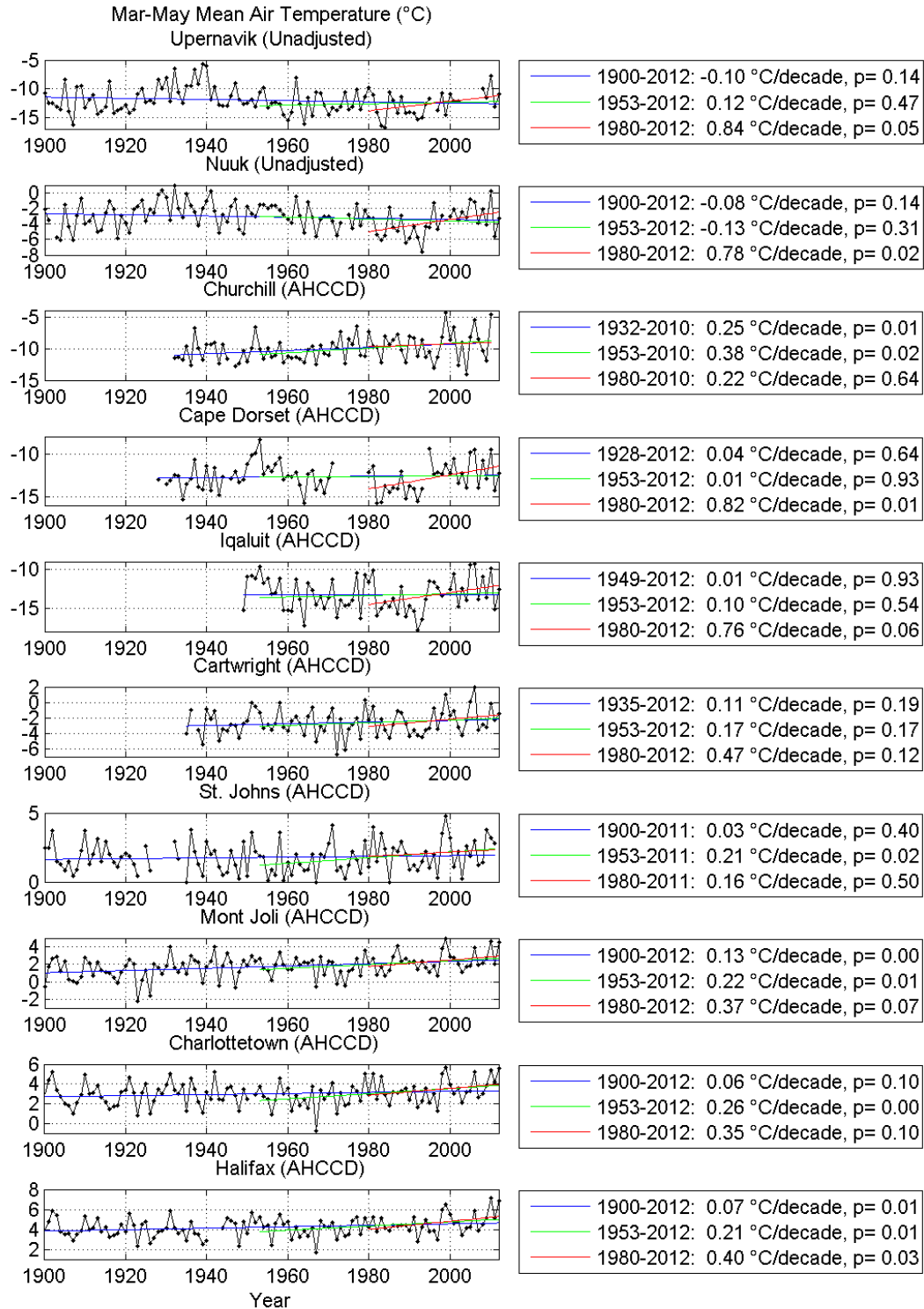


Fig. A1-5. Spring (Mar-May) mean air temperatures.

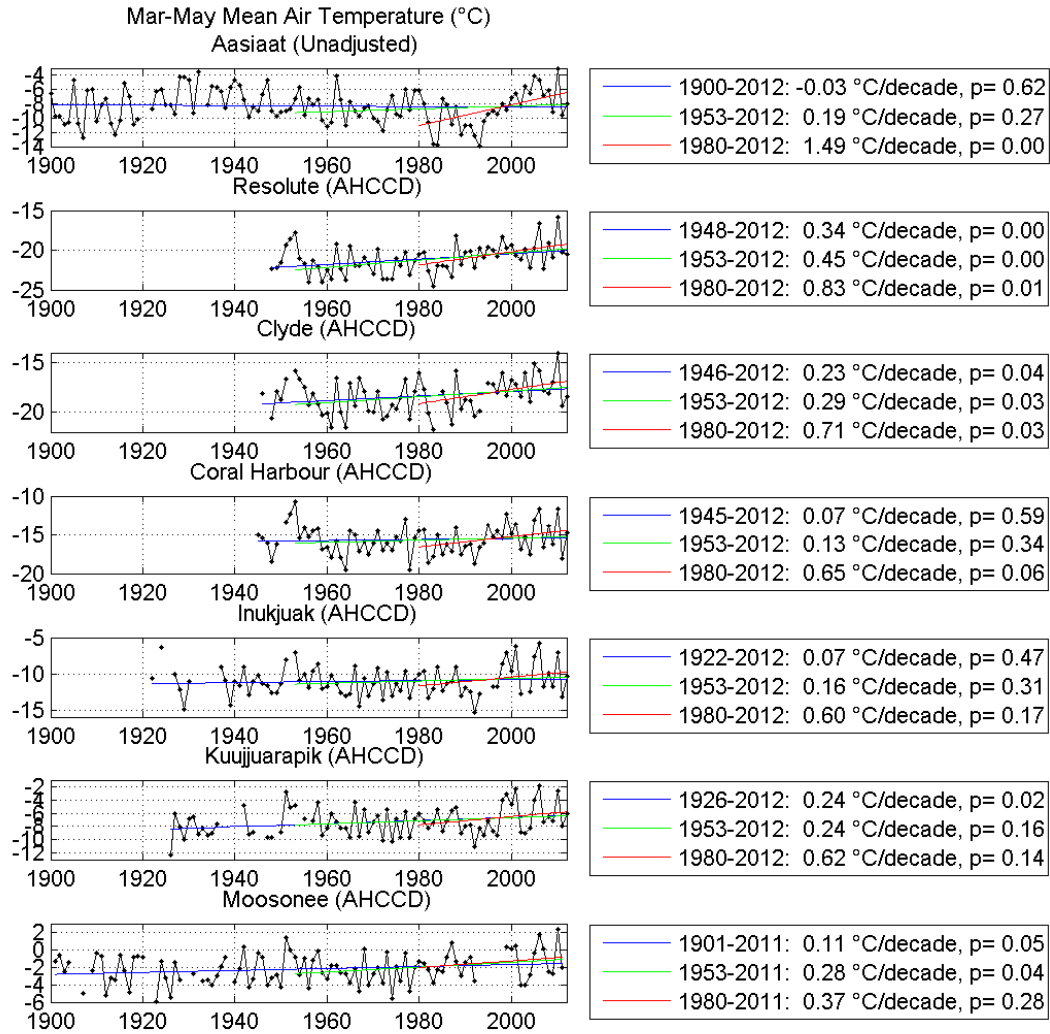


Fig. A1-5. continued.

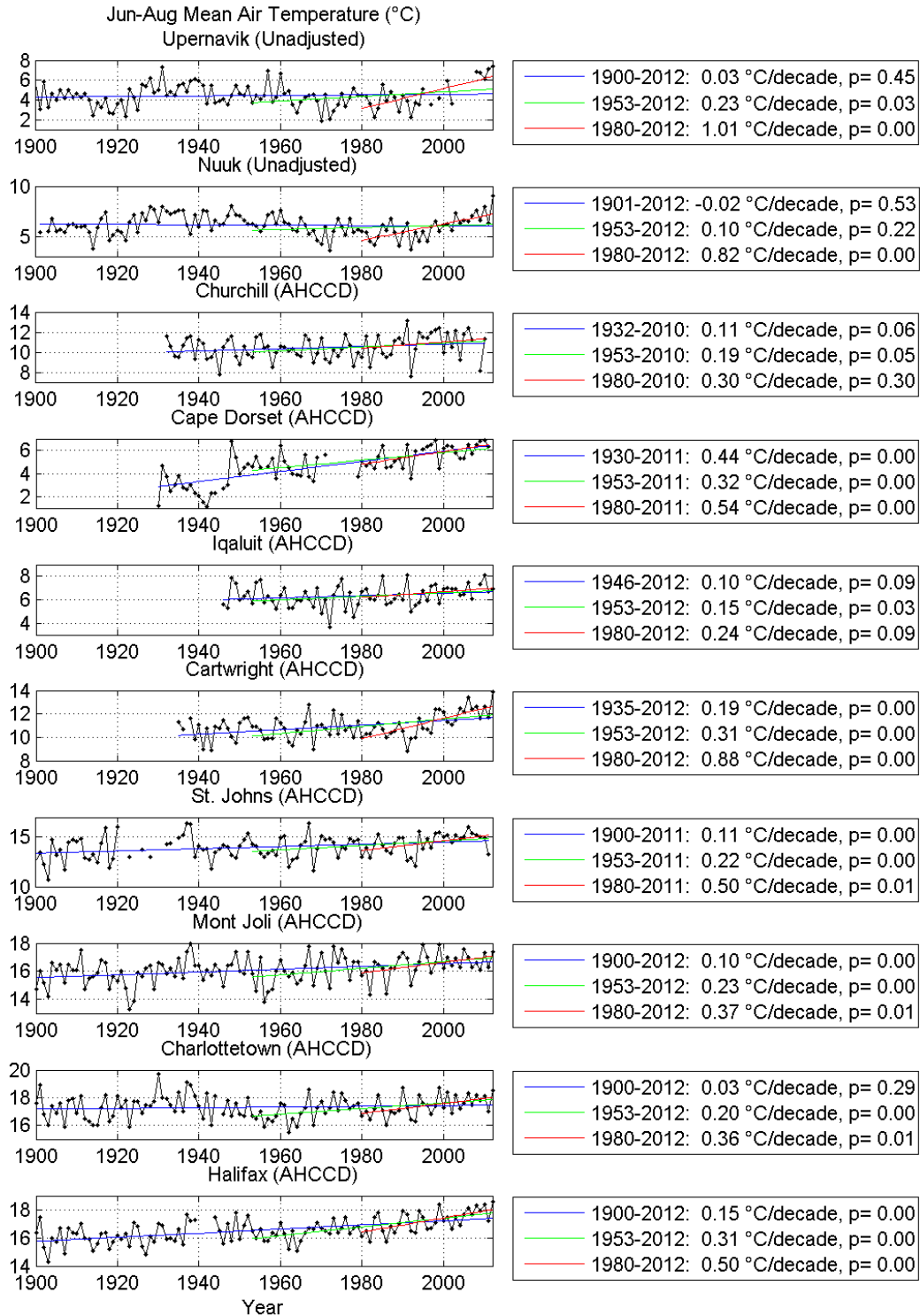


Fig. A1-6. Summer (Jun-Aug) mean air temperatures.

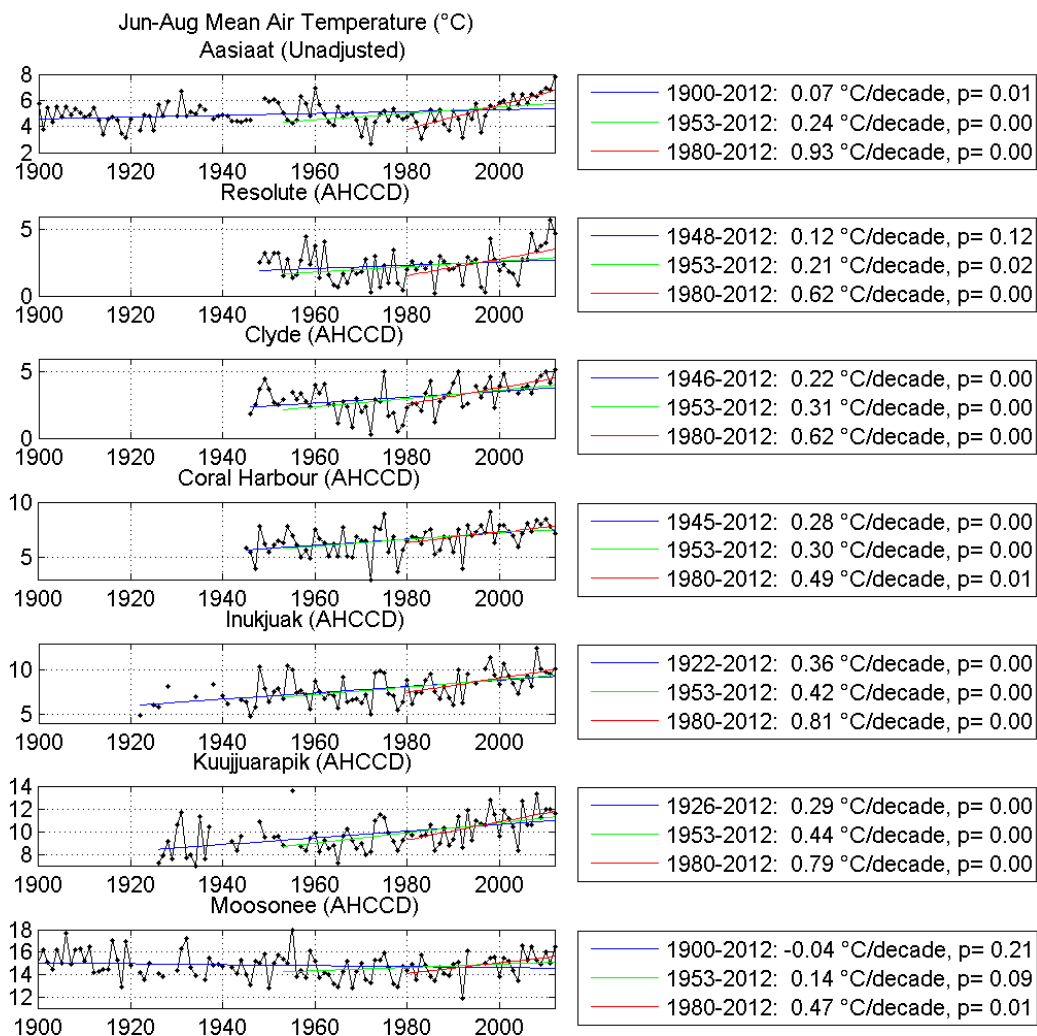


Fig. A1-6. continued.

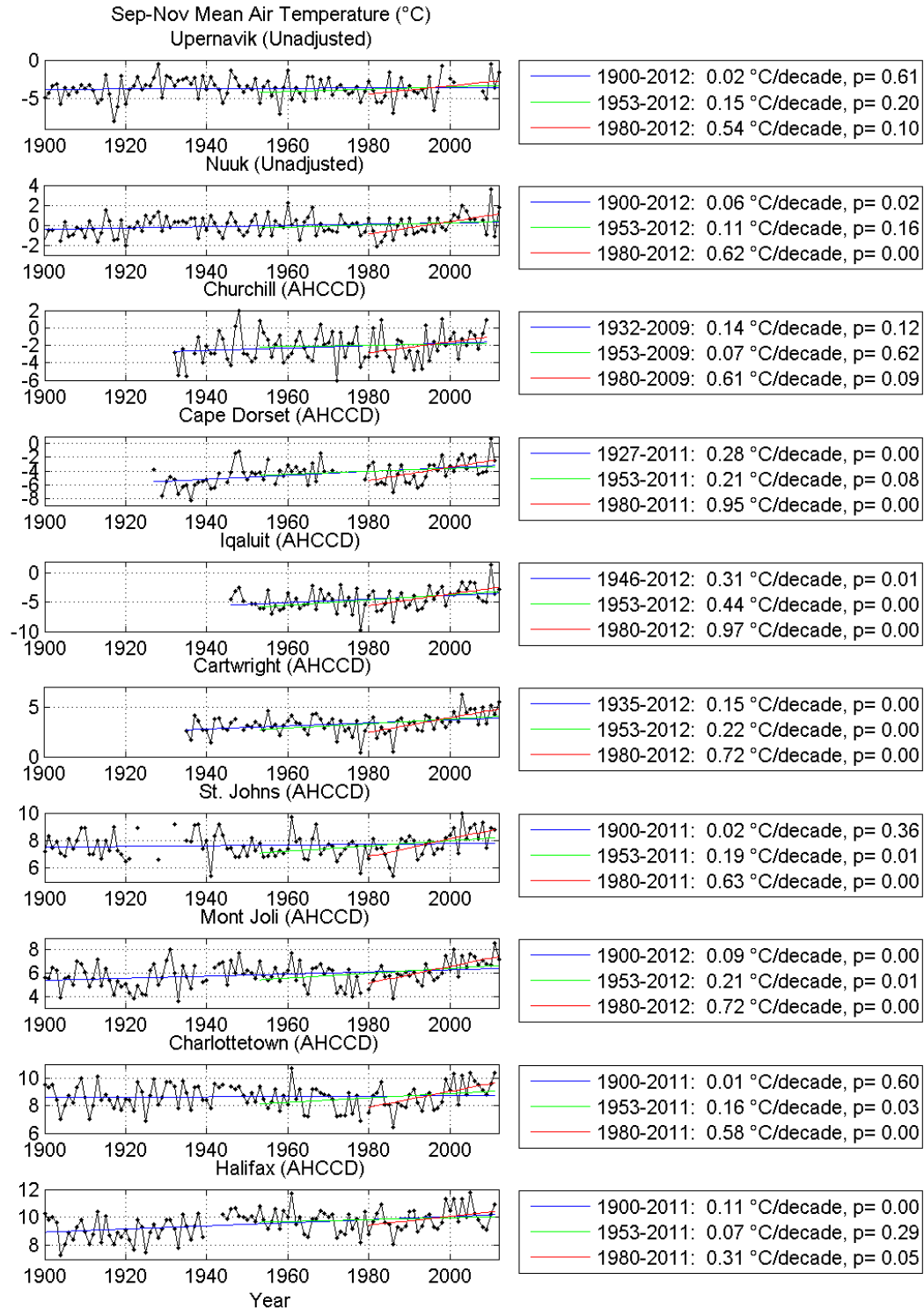


Fig. A1-7. Autumn (Sep-Nov) mean air temperatures.

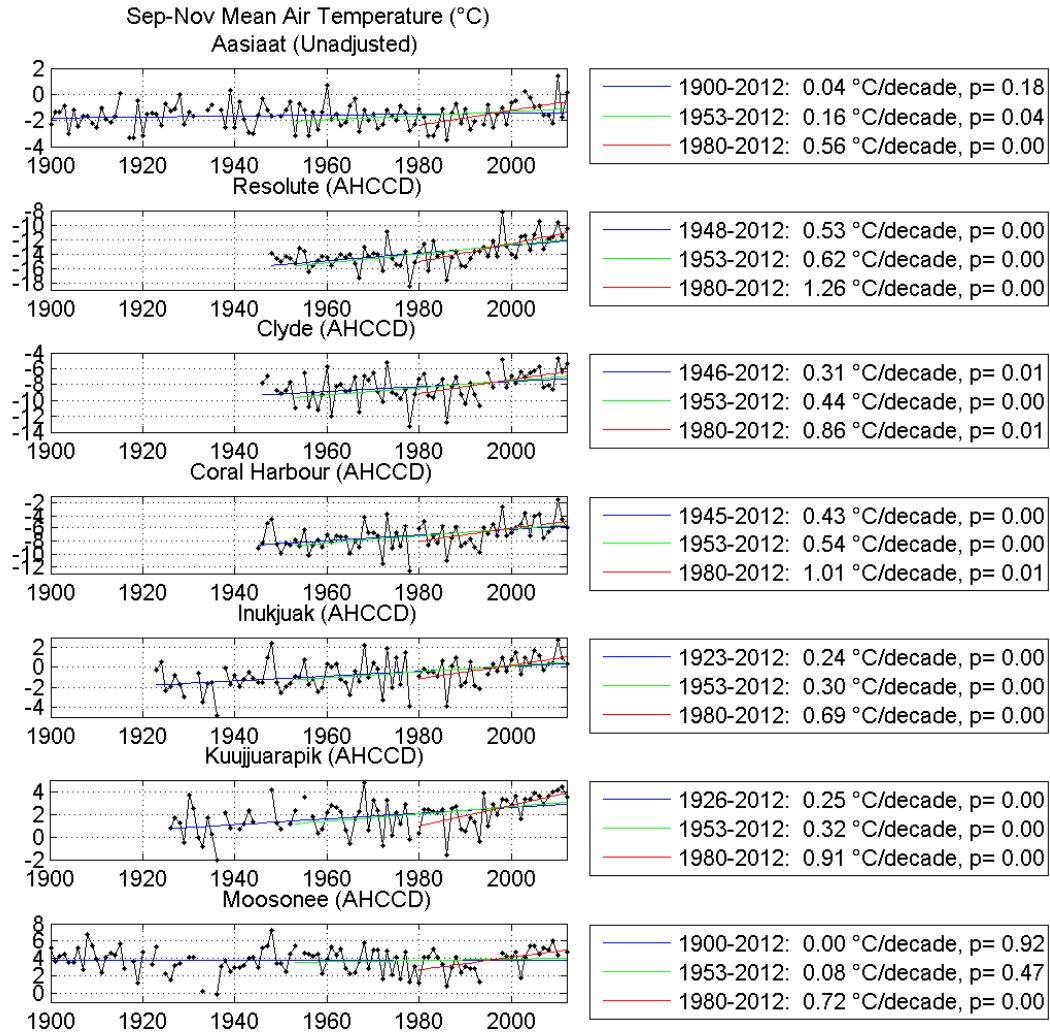


Fig. A1-7. Autumn (Sep-Nov) continued.

APPENDIX 2: EFFECT OF ICE DATA REPLACEMENT

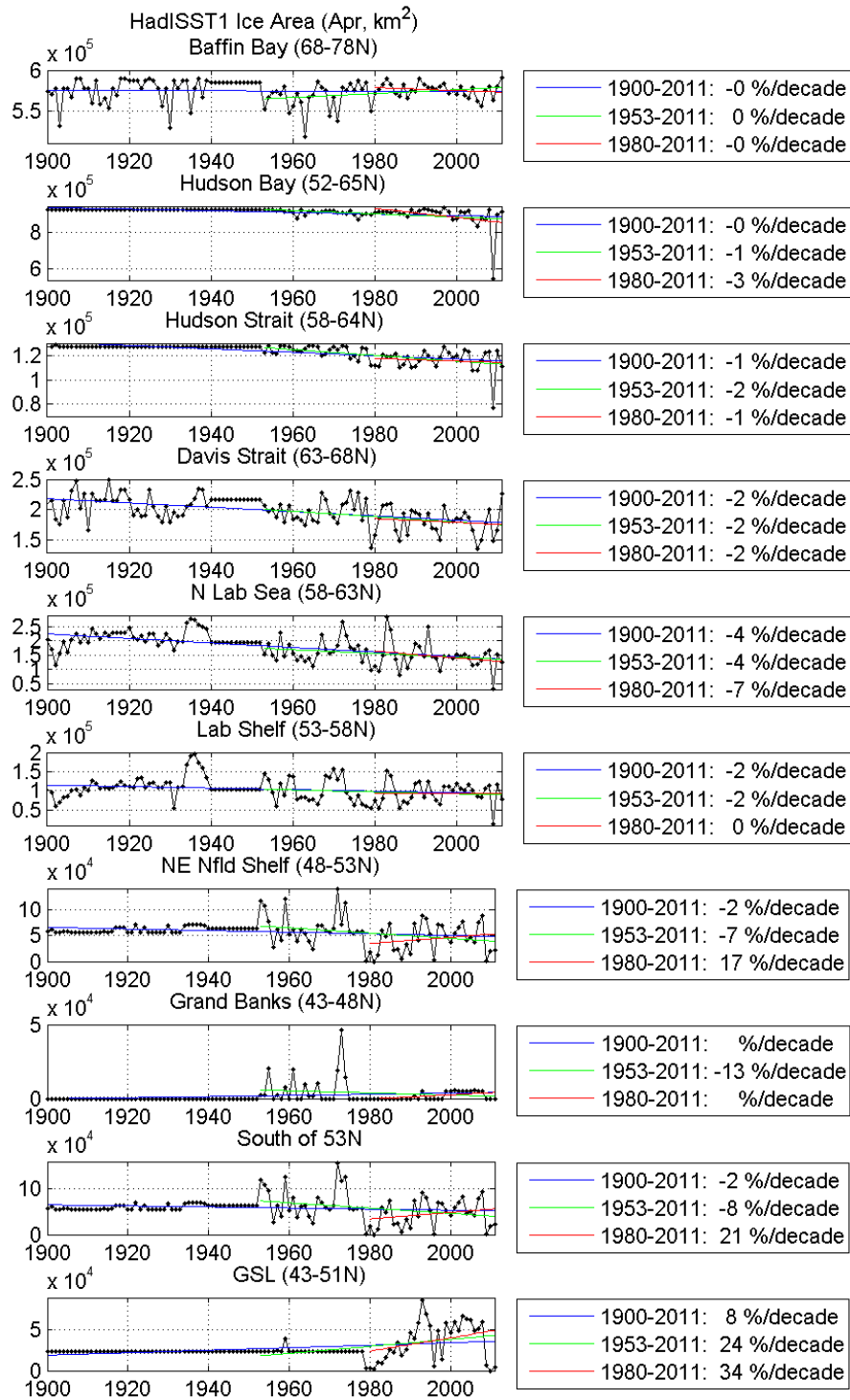


Fig. A2-1. Monthly ice concentrations from the HadISST1 dataset are plotted for several areas, generally from north to south for April.

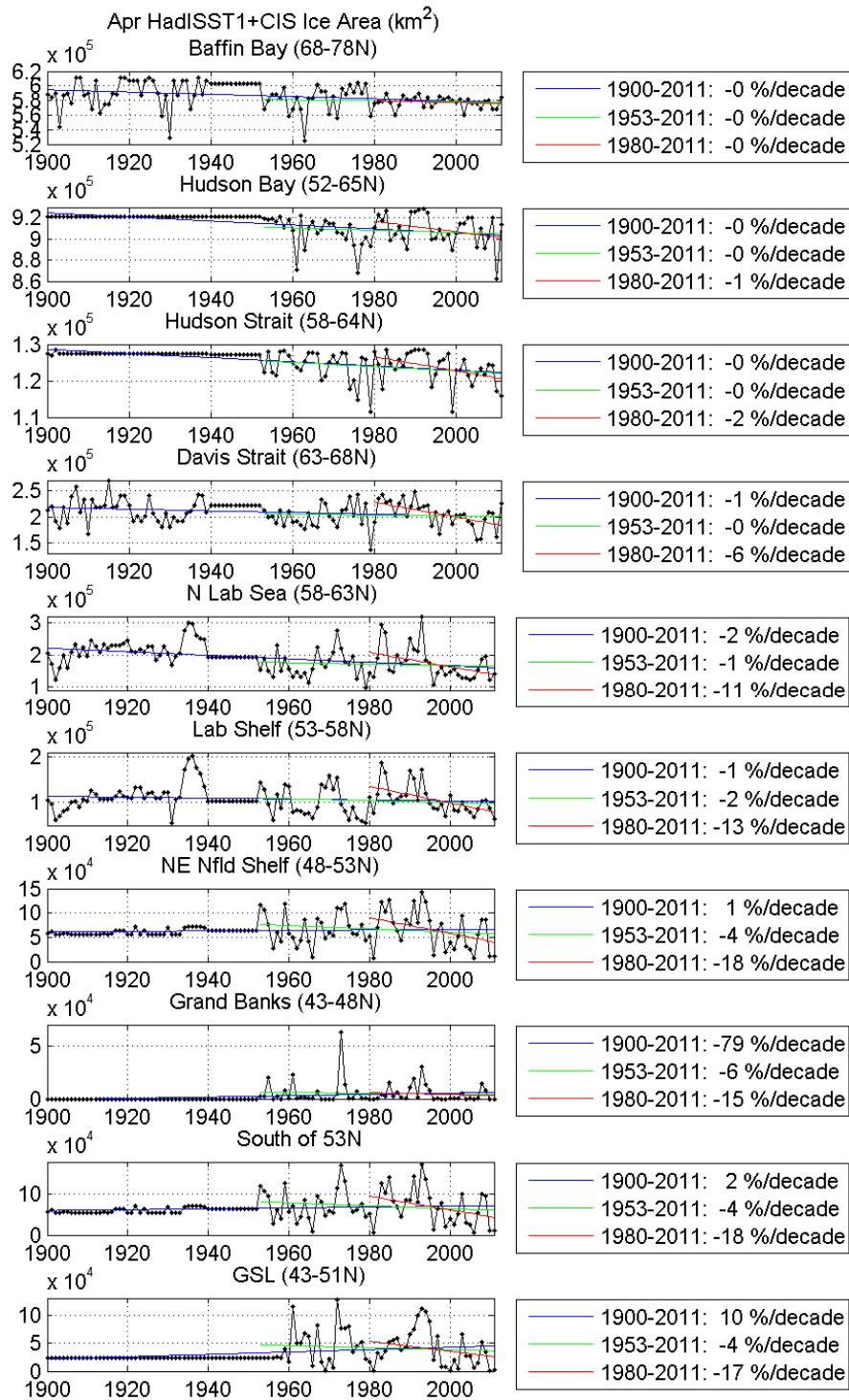


Fig. A2-2. HadISST1 data, with data after 1960 replaced with available CIS ice chart data.

APPENDIX 3. SEASONAL SEA ICE AREA TIME SERIES.

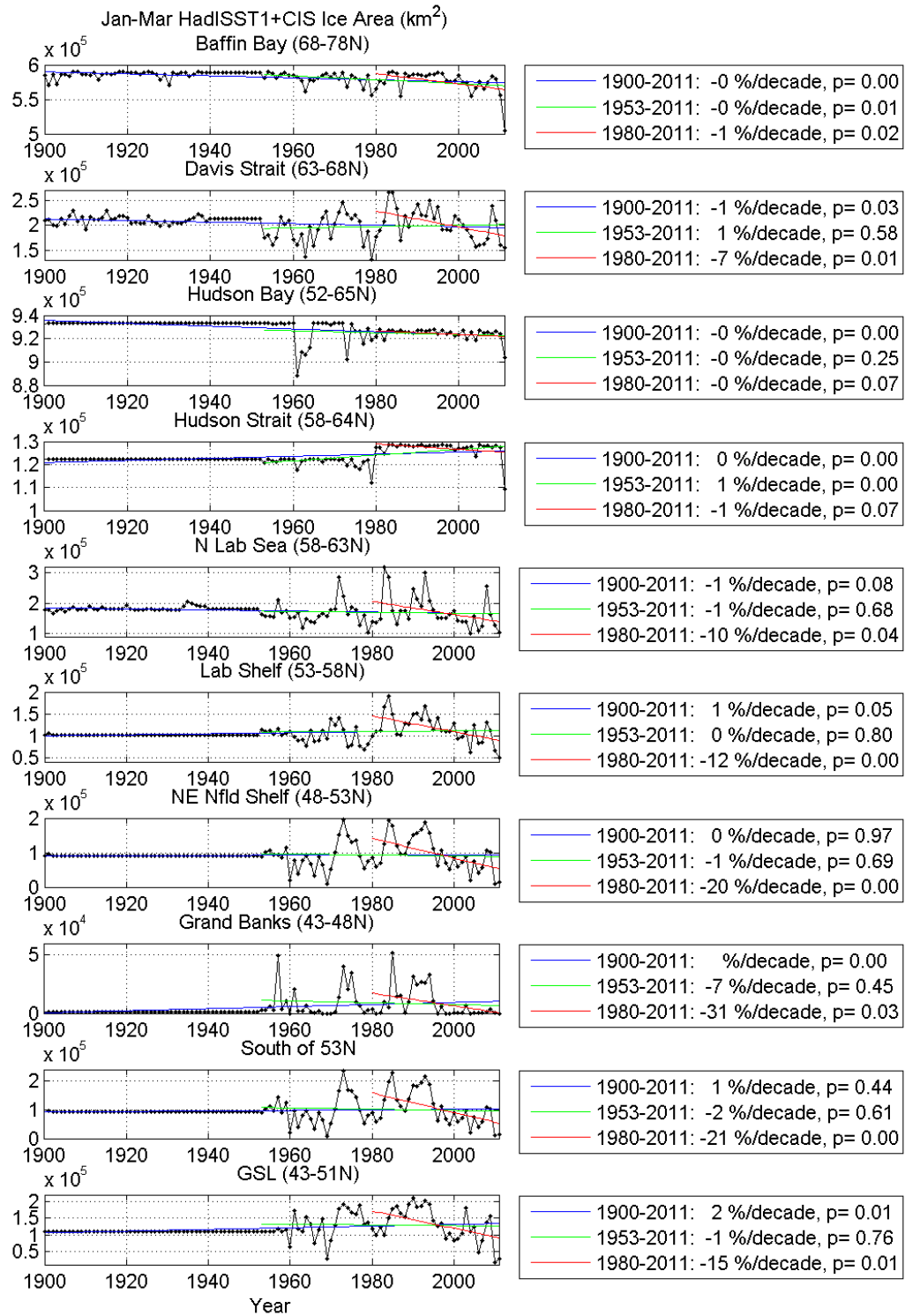


Fig. A3-1. Winter (Jan-Mar) mean ice area.

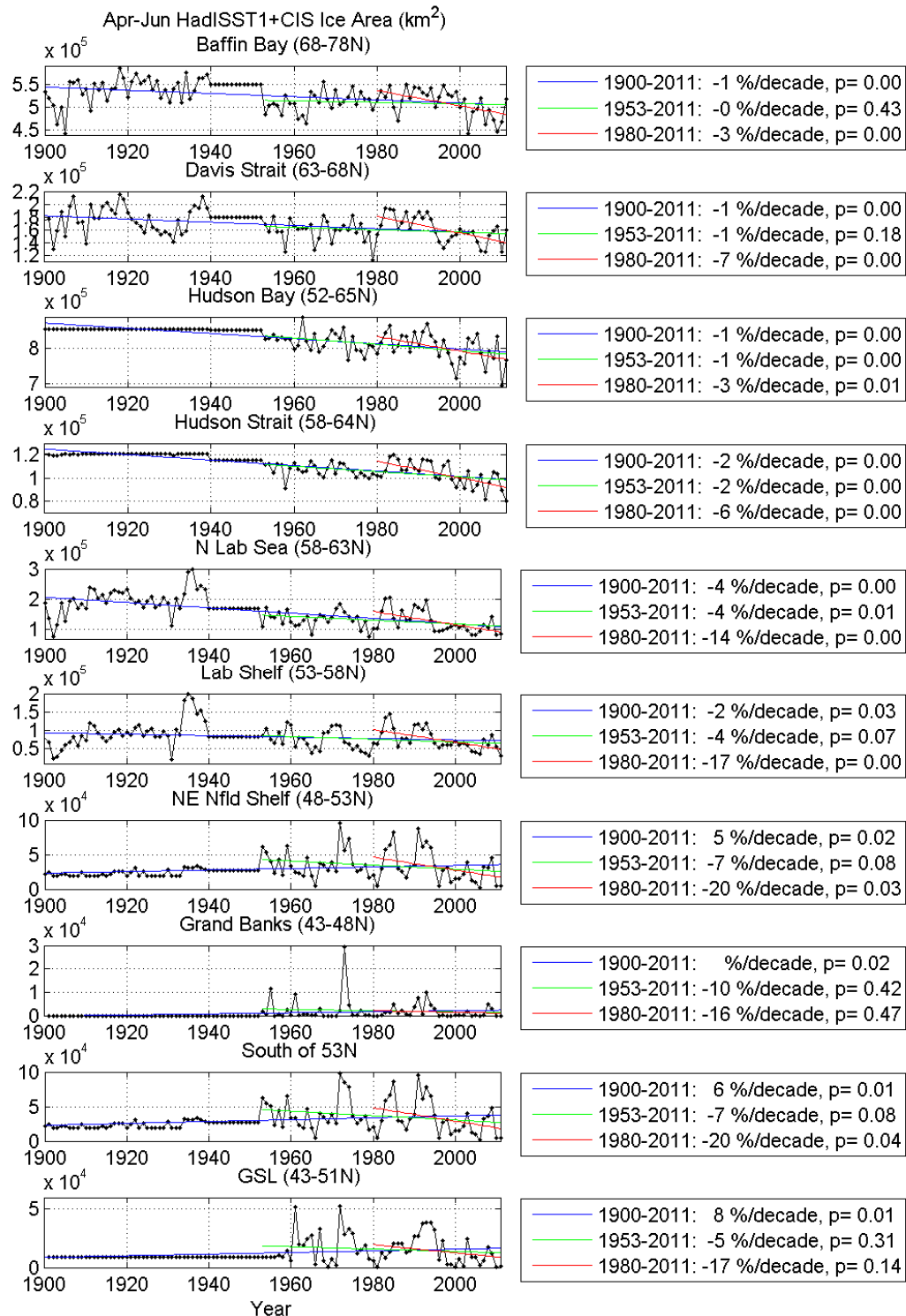


Fig. A3-2. Spring (Apr-Jun) mean ice area.

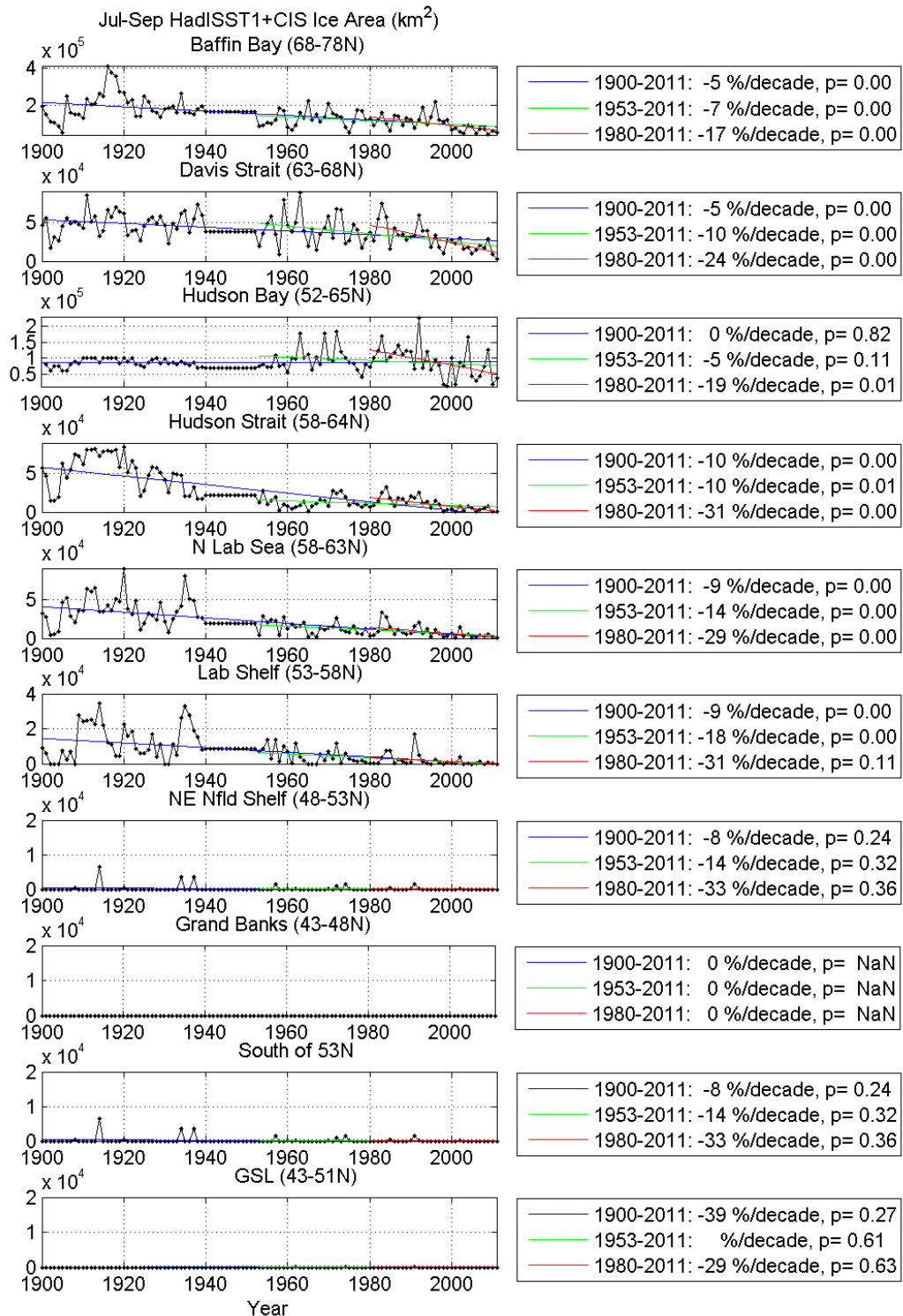


Fig. A3-3. Summer (Jul-Sep) mean ice area.

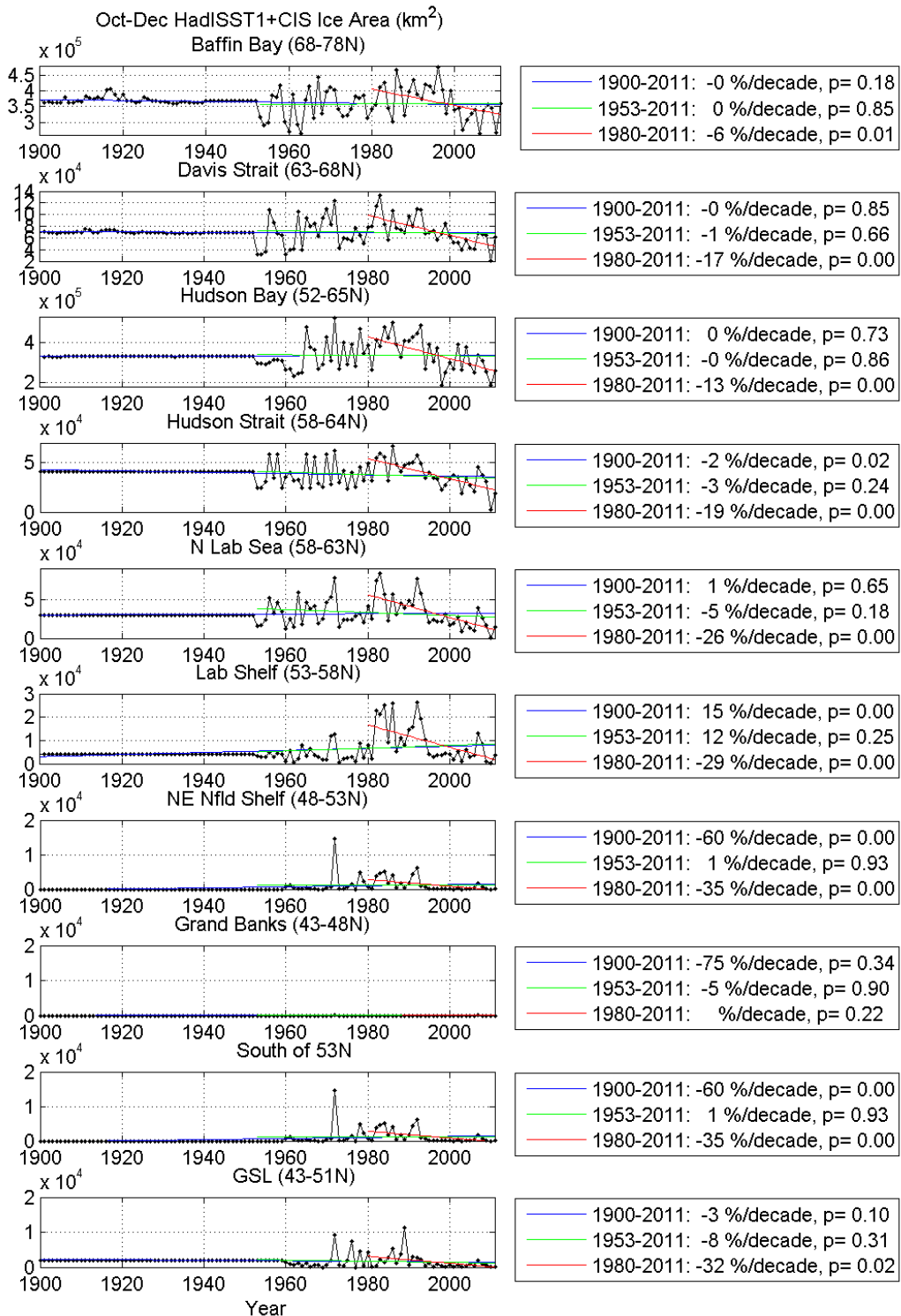


Fig. A3-4. Autumn (Oct-Dec) mean ice area.

APPENDIX 4. CLIMATE INDICES

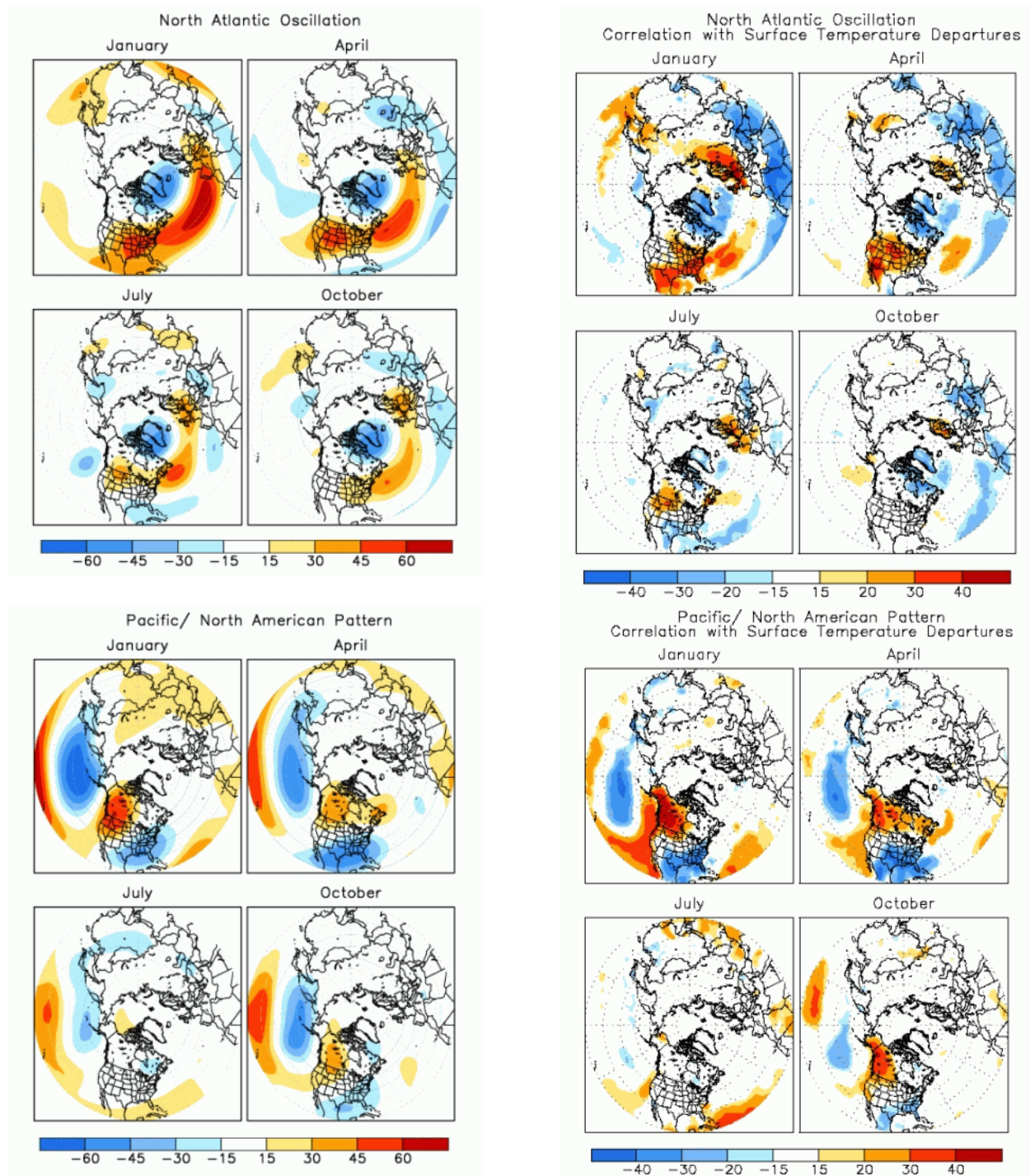


Fig. A4-1. Loading patterns (left) and correlations with surface temperature (right) for NAO, PNA, and EP-NP patterns, from NOAA National Weather Service Climate Prediction Center at <http://www.cpc.ncep.noaa.gov/data/teledoc/telecontents.shtml>.

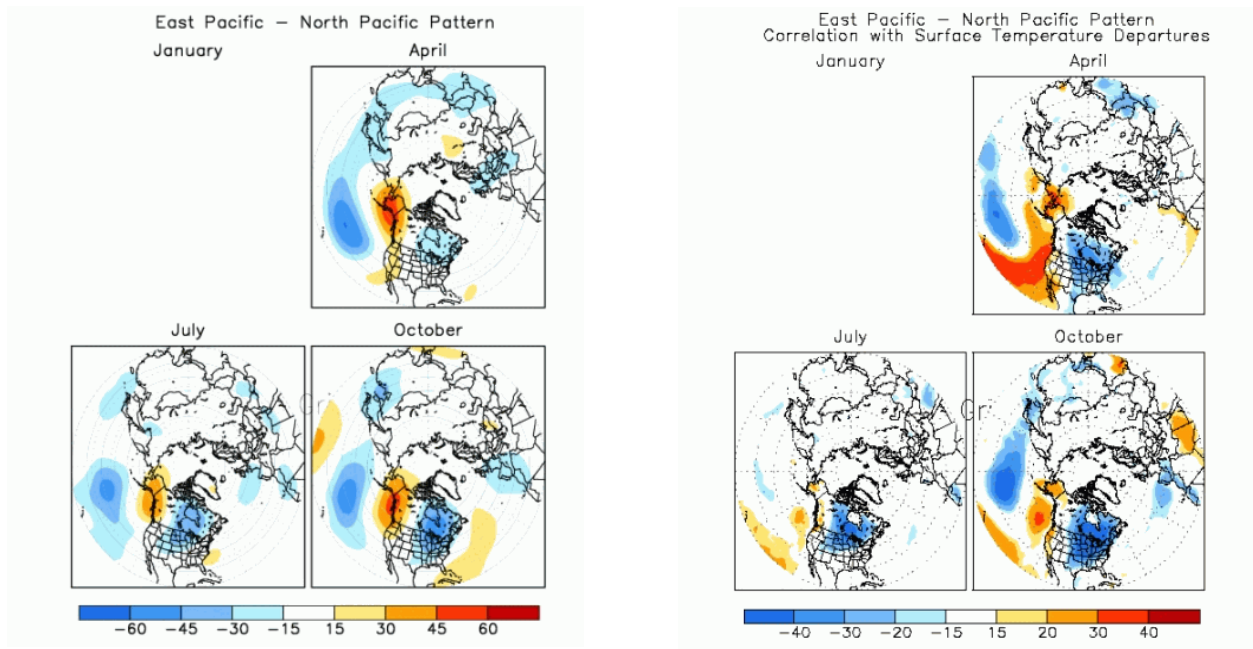


Fig. A4-1 (cont.)

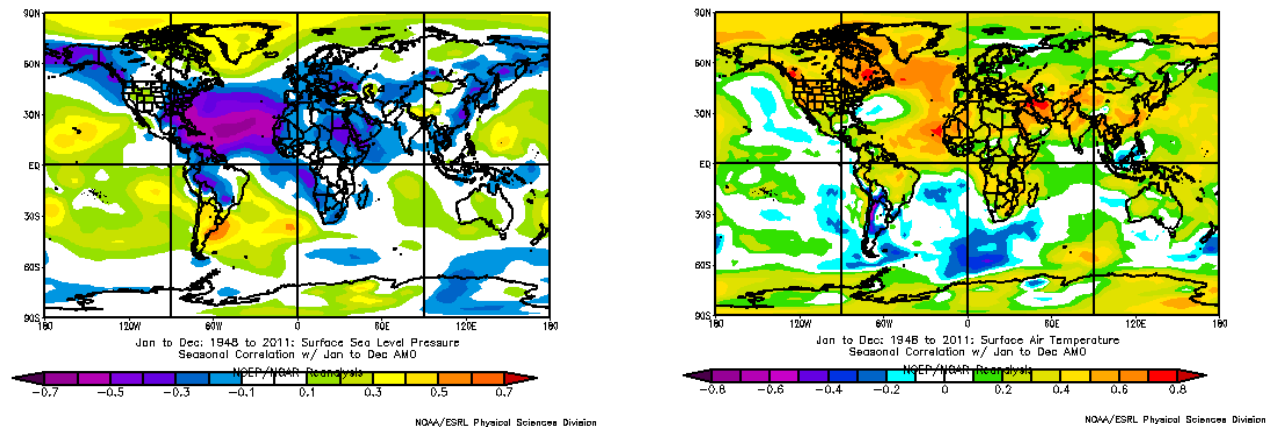


Fig. A4-2. Correlations of the AMO (Enfield et al., 2001) with SLP (left) and surface air temperature (right) using NCEP/NCAR Reanalysis dataset (Kalnay et al., 1996). Images provided by the NOAA/ESRL Physical Sciences Division, Boulder Colorado from their Web site at <http://www.esrl.noaa.gov/psd/>.